Thin–Walled Structures 160 (2021) 107391

Contents lists available at ScienceDirect

Thin-Walled Structures

journal homepage: http://www.elsevier.com/locate/tws

Spectral dynamic stiffness theory for free vibration analysis of plate structures stiffened by beams with arbitrary cross-sections

Xiang Liu [a,b,c], Yu Li [a,b], Yuliang Lin [a,d,*], J. Ranjan Banerjee [e]

[a] Joint International Research Laboratory of Key Technology for Rail Traffic Safety, Central South University, Changsha, 410075, China
[b] Key Laboratory of Traffic Safety on Track, Ministry of Education, School of Traffic & Transportation Engineering, Central South University, Changsha, 410075, China
[c] State Key Laboratory of High Performance Complex Manufacturing, Central South University, Changsha, 410075, China
[d] School of Civil Engineering, Central South University, Changsha, 410075, China
[e] School of Mathematics, Computer Science and Engineering, City University London, London, EC1V 0HB, UK

ARTICLE INFO

Keywords:
Spectral dynamic stiffness method
Beam stiffened plates
Closed-section and open-section beam stiffeners
Arbitrary boundary conditions
Wittrick-Williams algorithm

ABSTRACT

A spectral dynamic stiffness (SDS) model for plate assemblies stiffened by beams is proposed. The theory is sufficiently general where the plate assemblies can be subjected to any arbitrary boundary conditions (BCs), but importantly, the beam stiffeners can be of open or closed cross-sections, and maybe connected to plates with or without eccentricity. First, by using modified Fourier series, the SDS formulations for different beam stiffeners are developed based on their equations of motion for the most general case. Then, the beam stiffeners' SDS matrices are superposed directly onto those of the plate assemblies. Next, the reliable, efficient and robust Wittrick-Williams algorithm is applied for the modal analysis of the overall structure. Representative examples are provided to illustrate the accuracy and versatility of the method, where the proposed theory is extensively validated by the software ANSYS. The proposed method inherits all advantages of the previously developed SDS theory for plate structures, including high computational efficiency, accuracy, robustness in eigenvalue calculation and the versatility in modelling arbitrary BCs. The proposed theory extends the existing SDS theory substantially to cover a wide class of beam stiffened plate structures used in train bodies, ship hulls, aircraft fuselage and wings and many others.

1. Introduction

In rail transportation, mechanical, civil, aerospace, marine and other engineering fields, plate structures are widely used in their design. In order to improve the vibration performance and to enhance the load carrying capacity and also at the same time, achieving a lighter structure, stiffeners are often used to reinforce plate structures. The stiffeners in a plate structures are generally modelled as beams whose cross-sections can vary widely, e.g. angle, channel, Tee, I, L, hat, etc. In the design of the lightweight structure of stiffened plate structures, there are many design parameters such as the spatial arrangements of the stiffeners, the cross-sectional dimensions (e.g. beam depth and width) and geometries (e.g. closed or open sections). In particular, the free vibration analysis of beam stiffened plate structures, especially in the mid and high frequency range is of considerable importance. This is mainly because such structures generally exhibit the coexistence of both long-wavelength and short-wavelength characteristics which can be difficult to handle and thus can become a challenging problem. The long-wavelength vibrating beam stiffeners can be modelled relatively easily by using the Finite Element (FE) method [1] whereas the short-wavelength vibrating plates may require Statistical Energy Analysis (SEA) [2,3] models. However, in most of the commercial FE software that are numerically based, the modelling and remodeling processes are quite tedious and often time consuming, mainly because of the remeshment in the optimization process. The whole procedure therefore, may become inadequate and inefficient.

Researches on the analytical modeling for dynamic analysis of beam stiffened plate structures have been carried out to a great measure by many researchers and notably, they have made tremendous progress and achieved significant results over the years. However, there is still a long way to go because the existing design is conservative and generous and there are some deficiencies in the current research that need to be addressed. Some selected pertinent literature is reviewed here. Elishakoff and Sternberg [4] reformulated the eigenfrequency problem by

* Corresponding author. Joint International Research Laboratory of Key Technology for Rail Traffic Safety, Central South University, Changsha, 410075, China.
E-mail addresses: xiangliu06@gmail.com (X. Liu), csuliyu@csu.edu.cn (Y. Li), linyuliang11@163.com (Y. Lin), j.r.banerjee@city.ac.uk (J.R. Banerjee).

https://doi.org/10.1016/j.tws.2020.107391
Received 29 June 2020; Received in revised form 2 November 2020; Accepted 16 December 2020
Available online 11 January 2021

determining the wavenumber of stiffened plates subject to simply-supported edges with three different forms of the eigenfrequency wavenumber. However, their research was confined to an individual isotropic rectangular thin plate stiffened along two parallel sides and simply supported along the other two sides. Mace [5,6] proposed a method for the dynamic vibration analysis of plates with two sets of parallel stiffeners when subjected to point excitations on the stiffeners. In their research, stiffened plates were used as the bulkheads and intermediate frames of a hull structure. Fourier wavenumber transform was used to obtain the steady-state response of the plate and the corresponding phase, but the effect of the beam stiffener was not studied which of course, may lead to unacceptably bad results. Mead [7] expanded the response expression of the stiffener in terms of discrete wave harmonics of the plate, and essentially he solved the vibration problem of an infinite plate reinforced by periodic stiffeners. The solution of the plate vibration and associated pressure field were effectively represented by the motion of the wave. When compared with Mace's approach [5,6], Mead's method simplifies the calculation process and improves the calculation efficiency. Yin et al. [8] studied the dynamic response of composite laminates periodically reinforced by stiffeners based on the previous work of Mace [6]. The reaction force was expressed as a function of the stiffener's dynamic stiffness and vibration velocity, but the effect caused by the eccentric beam connection was not taken into consideration. Siddiqi and Kukreti [9] considered the in-plane force of the plate, the axial stiffness of the stiffener, the interaction between the beam and the plate due to eccentricity, and the torsional and shear stiffnesses of the beam, and they proposed a differential quadrature method for eccentric stiffened plates under a single lateral load. Mittelstedt [10] devoted to the analysis of orthotropic plates under uniaxial uniform compressive load. The plates under consideration were stiffened by open-section stiffeners in the longitudinal direction. However, their analysis was limited to certain boundary conditions. Li and his coauthors [11,12] proposed an analytical method for the vibration analysis of plates stiffened by any number of beams with any length and any arrangement angle. This method represents each displacement function as a modified version of Fourier series, which consists of a standard Fourier cosine series and several supplementary functions. In this method, both the beam and plate are modelled by the Rayleigh-Ritz method, which is applicable to a range of stiffened plates vibration problem with different boundary conditions, but the modeling of extra stiffeners would no-doubt become extremely tedious. Lin [13] proposed an analytical method for solving the vibration response of ribbed plates with clamped boundaries by using traveling wave solutions. The dependency of the dynamic response of the ribbed plate was studied through experiments by the same author [13]. Later, Lin and Zhang [14] analyzed the vibration response of ribbed plates with free boundary conditions. They used the double cosine integral transformation technique to arrive at the analytical solution when investigating the free and forced vibration of ribbed plates. However, in their work neither different types of cross-sections nor the eccentricity of the stiffening beam to the connecting plate was considered. Also, the investigators focused only on an individual plate with special boundary conditions rather than as assembly of plates. Golkaram and Aghdam [15] proposed a solution for free transverse vibration of a rectangular thin plate suspended locally on a deformable beam by using generalized differential quadrature method. The plate was completely free at all edges except for the local area connected to a beam with a rectangular cross-section. However, this investigation considered only lateral vibration and the beam structure was relatively simple. On another hand, Gorman [16] used the superposition method to obtain the analytical solution for the free vibration analysis of an individual plate whose edges are stiffened by, however, non-eccentric beam stiffeners. Zheng and Wei [17] carried out a vibration analysis of a bidirectional stiffened thin plate with non-uniform discrete elastic boundary constraints. They applied energy method to derive governing equation of motion of the stiffened plate, and then they used a series of simple polynomials and boundary constraints that meet the Rayleigh-Ritz convergence criterion to discretize the governing equation. However, they did not consider different cross-sections of the beam stiffeners. Aksogan et al. [18] used the continuous connection method (CCM) and Vlasov's thin-walled beam theory to solve the stiffness matrix of the structure, and performed a dynamic analysis of the non-planar asymmetric coupled shear wall on a rigid foundation. Of course, there are other analytical work on the buckling and vibration of thin-walled structures such as membranes [19,20], plates [21–23] and shells [24–26], where stiffener is absent.

As reviewed above, most of the research either focuses only on a simple plate structure with simple boundary condition or relies on using many DOFs to model the structure which makes the method computationally inefficient. The dynamic stiffness method (DSM) is a powerful and robust method suitable for analysis of beam-stiffened-plate structures using very few DOFs, while preserving very high accuracy of the results. The DSM adopts exact shape functions ensuring its accuracy within all frequency ranges by using very few DOFs. The individual elements in DSM are frequency dependent, having both mass and stiffness properties, and thus the method allows a straightforward assembling procedure for complex structures, even for multibody systems [27]. Wittrick and Williams [28] are probably the first to develop the DSM for plated structures with an opposite pair of edges simply supported (Levy-type plates). Boscolo and Banerjee [29] derived the dynamic stiffness matrix of Levy-type plates and their assemblies by enhancing the work of Wittrick and Williams [28]. Tounsi et al. [30] and Fazzolari [31] proposed dynamic stiffness solutions for the bending vibration of axisymmetric stiffened shells and doubly curved laminated shells, respectively. Li et al. [32] used the projection method to project the forces on the plate nodes and their corresponding displacements onto a set of orthogonal functions, overcoming the known space-dependent difficulties, and thereby establishing a formula for calculating the dynamic stiffness of the plate in bending vibration of with simply supported boundary conditions. More recently, Liu et al. [33] proposed the DS formulations for membranes and their assemblies with general classical boundary conditions. In a recently published paper, Liu et al. [34] further developed the DS formulations for plate assemblies with a pair of opposite edges having all possible combinations of simple supports and guided supports.

The DSM has been used to model beam-stiffened plate structures rather sporadically. For instance, Langley [35] established a formula for calculating the dynamic response of plates with transversely added beams and subjected to longitudinally simply supported boundary conditions, but he ignored the in-plane motion of the beam stiffened plate. Later, in a different context, Langley [36] took the in-plane motion into consideration, and analyzed the dynamic response of stiffened shell structure. Watson et al. [37] used Lagrangian multipliers to model point supports of Levy-type plates based on exact strip method, and thus they performed vibration and buckling analysis of stiffened panels. Yin et al. [38] proposed a dynamic stiffness model for eccentrically beam-stiffened plates. However, it is apparent that most of the above studies are restricted to plate structures with at least one pair of opposite edges of the plate being simply supported, and the elements can be assembled only in one direction. This is indeed a serious limitation for the application of the theory to practical structures.

In order to remove the above restrictions in the literature, many researchers have proposed different dynamic stiffness models in recent years [39–51]. Some of these models are applicable to plate elements with more general boundary conditions, and the elements can be assembled in two directions. Amongst these contributions, Liu, Banerjee and their coauthors [33,34,39–47,51] proposed the spectral dynamic stiffness method (SDSM) for both the transverse [33,34,39–42,51] and inplane [43] vibration problem of the plate by combining the spectral method with the classical dynamic stiffness method for plate with classical boundary conditions (BCs) and non-classical BCs [44,45]. The method has also been extended to buckling analysis of plates [46,47]. Nefovska-Danilovic and her coauthors proposed dynamic stiffness

matrices for plate elements with general boundary conditions for the in-plane vibrations [48] and transverse vibrations based on the first-order deformation theory [49] and higher-order deformation theory [50]. Although the above researches have removed previous restrictions to a great extent, but still, there is no reported research for DS models of plate assemblies with general boundary conditions, particularly stiffened by beams with complex open and closed sections.

The main purpose of this paper is to extend the Spectral Dynamic Stiffness (SDS) [26,29] theory to beam stiffened plate structures with general boundary conditions beam stiffeners having complex cross-sections. First, the general framework of the SDS method is reviewed. Then, the governing differential equations which represent the free vibration behaviour of both open-section and closed-section beam stiffeners are formulated. Subsequently, the SDS formulation of different beam stiffeners are developed by using the modified Fourier series. The beam stiffeners' SDS matrices are then superposed directly to those of the plate assemblies without resorting to other rather cumbersome techniques such as penalty method or Lagrangian Multipler method. The efficient and robust algorithm of Wittrick and Williams [28] is invoked and the so-called *J0* count has already been resolved in this paper when computing the natural frequencies [26,29]. The proposed method retains all advantages of the SDSM [26,29] and it extends the application scope by covering more general beam stiffened plate structures.

This paper is organized as follows. First, the general framework and some properties of SDSM are briefly reviewed in Section 2.1, and then the SDS matrices of open-section beam stiffener and closed-section beam stiffener are derived in Section 2.2. Next, Section 2.3 describes the assembly procedure of the SDS formulations of beam stiffeners and plate structures. This is followed by Section 3 in which the proposed SDSM is validated with the help of the commercial FE software ANSYS and computing a range of representative beam stiffened plate structures. Finally, significant conclusions are drawn in Section 4.

2. Theory

An important feature of this paper is to extend the generality as well as the versatility of the SDSM when applied to stiffened plate structures. This section summarizes the framework and characteristics of SDSM, derives the SDS matrices of beam stiffeners with complex cross-section and describes the assembly procedure of the overall SDS matrix of the beam stiffened plates structures.

2.1. Framework of the spectral dynamic stiffness method

One of the key points of SDSM used here is the application of modified Fourier series [35,42]. For any displacement or force boundary condition, the modified Fourier series along a plate edge is given by

$$h(\xi)=\sum_{\substack{s\in N\\ l\in\{0,1\}}} H_{ls}\frac{\mathscr{T}_l(\gamma_{ls}\xi)}{\sqrt{\zeta_{ls}L}},\quad H_{ls}=\int_{-L}^{L}h(\xi)\frac{\mathscr{T}_l(\gamma_{ls}\xi)}{\sqrt{\zeta_{ls}L}}\mathrm{d}\xi \tag{1}$$

where $N=\{0,1,2,\ldots\}$ is the non-negative integer set, and 'l' takes the value of either '0' or '1' to represent the corresponding symmetric or antisymmetric functions. The constant ζ_{ls} is given as

$$\zeta_{ls}=\begin{cases}2 & l=0 \quad \text{and} \quad s=0\\ 1 & l=1 \quad \text{or} \quad s\geqslant 1\end{cases} \tag{2}$$

The definition of the Fourier series $\mathscr{T}_l(\gamma_{ls}\xi)$ in Eq. (1) is defined as

$$\mathscr{T}_l(\gamma_{ls}\xi)=\begin{cases}\cos\left(\dfrac{s\pi}{l}\xi\right) & l=0,\\ \sin\left(\left(s+\dfrac{1}{2}\right)\dfrac{\pi}{l}\xi\right) & l=1\end{cases},\quad \xi\in[-L,L],\quad s\in N \tag{3}$$

By using the modified Fourier series, the general solution of the governing differential equations (GDE) of a plate element in the frequency domain can be developed within the spectral dynamic stiffness framework. After considerable algebraic operations, the dynamic stiffness matrix of a plate for general BC can be derived with the help of the modified Fourier series defined above. The final matrix expressions are available in the Appendix, but interested readers are referred to Refs. [26,29] for further details. With the above pretext, the theory is briefly explained as follows.

The force $f(\xi)$ and displacement $d(\xi)$ boundary conditions on the ith line node take the following form

$$\boldsymbol{f}_i=[F_{i00},F_{i01},F_{i02},\ldots,F_{i10},F_{i11},F_{i12},\ldots]^T$$
$$\boldsymbol{d}_i=[D_{i00},D_{i01},D_{i02},\ldots,D_{i0},D_{i11},D_{i12},\ldots]^T$$

where F_{ils} and D_{ils} are respectively the modified Fourier (MF) coefficients of the corresponding force and displacement boundary condition applied on the ith line nodes, obtained by applying Eq. (1) onto $f(\xi)$ and $d(\xi)$.

The relationship between overall force and displacement is expressed as

$$\boldsymbol{f}=\boldsymbol{K}\boldsymbol{d}$$

where $\boldsymbol{K}$ is the SDS matrix of the plate element, which links the modified Fourier coefficient vector of force $f(\xi)$ to the displacement $d(\xi)$ at all line nodes (plate boundaries). For the ith line node, the relationship between the MF coefficients of force and displacement boundary condition can be defined as

$$\boldsymbol{f}_i=\boldsymbol{K}_{ii}\boldsymbol{d}_i$$

2.2. Spectral dynamic stiffness formulations for beam stiffeners

For the vibration analysis of plate structures stiffened by beam stiffeners, several factors need to be addressed. For instance: different cross-sections of beam stiffeners, different shapes, with or without eccentricity, etc. The current research considers the combination of plates with beams of different cross-sections, shapes and eccentricity.

2.2.1. SDSM of the open-section beam stiffener

Fig. 1(a) shows a schematic view of a plate stiffened by an open-section beam stiffener. The analysis of the structure shown includes the effect of a force (prestress) T acting along the stiffener. Note that T is positive when tensile. The beam section is connected to the plate at point P, while C and S represent the centroid and shear center respectively at the beam stiffener. The connection point P and shear center S are on the same vertical plane. Parameters c_0 , c_1 and c_2 are the offsets among points S, P and C as shown in Fig. 1(a). The rotation angle of the stiffener is denoted by parameter ψ, and the displacements of points S, P and C are written as (w_0,μ_0), (w,μ) and (w_c,μ_c) respectively. The forces acting on various points of the stiffener are shown in Fig. 1(b) $EI\Gamma$ represents warping constant and GJ is torsion constant, EI_1 ,EI_2 and EI_{12} are the bending stiffness of the structure; ρA and I are the mass and polar moment of inertia per unit length. Q, H and M are the reaction forces on the plate boundary. The relationship between the displacements and rotation angles of those points can be expressed as $\mu_0=\mu-c_0\psi$, $w_0=w$, $\mu_c=\mu+c_1\psi$and $w_c=w+c_2\psi$. Under this premise, considering the balance of forces and moments with respect to the shear center, and making $\mu=0$(assuming that the plate is an effective rigid plane within the frequency range considered, without plane motion), one may arrive at the following governing differential equations for the beam stiffener,

$$\begin{aligned}EI\Gamma\psi^{iv}-\left[GJ+T\left(c_1{}^2+c_2{}^2+c_1c_0\right)\right]\psi''+\left[I+\rho A\left(c_1{}^2+c_2{}^2+c_1c_0\right)\right]\ddot{\psi}\\ -c_2Tw''+c_2\rho A\ddot{w}-M-Hc_0=0\end{aligned} \tag{4}$$

$$EI_1w^{iv}-Tw''+\rho A\ddot{w}-EI_{12}c_0\psi^{iv}-c_2T\psi''+c_2\rho A\ddot{\psi}-Q=0 \tag{5}$$

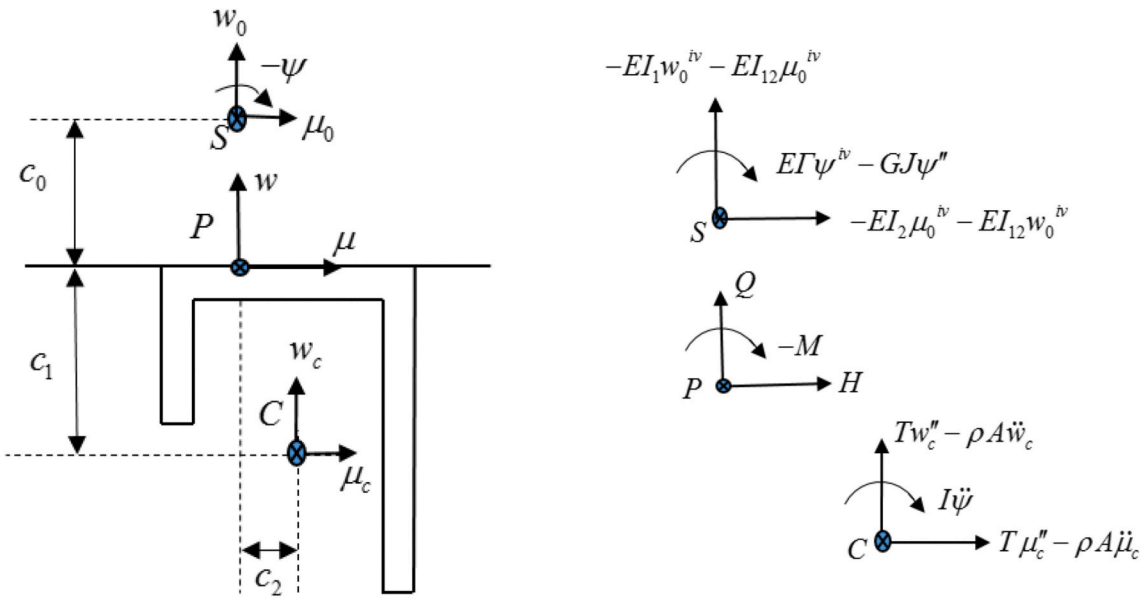

(a) Assembly diagram (b) Force diagram

Fig. 1. An open-section beam stiffener.

$$EI_{12}w^{iv} - EI_2c_0\psi^{iv} - c_1T\ddot{\psi} + c_1\rho A\ddot{\psi} - H = 0 \tag{6}$$

Combining Eqs. (4) and (6) and eliminating H, we have

$$(E\Gamma + EI_{12})\psi^{iv} - EI_{12}c_0w^{iv} - \left[GJ + T\left(c_1^2 + c_2^2\right)\right]\psi'' + \left[I + \rho A\left(c_1^2 + c_2^2\right)\right]\ddot{\psi} - c_2Tw'' + c_2\rho A\ddot{w} - M = 0 \tag{7}$$

Transforming Eqs. (5) and (7) from time domain to frequency domain gives

$$EI_1w^{iv} - Tw'' - \rho Aw^2 - EI_{12}c_0\psi^{iv} - c_2T\psi'' - c_2\rho Aw^2\psi - Q = 0 \tag{8}$$

$$(E\Gamma + EI_{12})\psi^{iv} - EI_{12}c_0w^{iv} - \left[GJ + T\left(c_1^2 + c_2^2\right)\right]\psi'' - \left[I + \rho A\left(c_1^2 + c_2^2\right)\right]w^2\psi - c_2Tw'' - c_2\rho Aw^2 - M = 0 \tag{9}$$

According to the theory of SDSM, we can express w, ψ, Q, M as the modified Fourier series form shown in Eq. (1),

$$\begin{cases} w(\xi) = \sum w_{ls}\dfrac{\mathscr{T}_l(\gamma_{ls}\xi)}{\sqrt{\zeta_{ls}L}}, & \psi(\xi) = \sum \psi_{ls}\dfrac{\mathscr{T}_l(\gamma_{ls}\xi)}{\sqrt{\zeta_{ls}L}} \\ s \in N \quad l \in \{0,1\} & s \in N \quad l \in \{0,1\} \end{cases} \tag{10a}$$

$$\begin{cases} Q(\xi) = \sum Q_{tr}\dfrac{\mathscr{T}_t(\gamma_{tr}\xi)}{\sqrt{\zeta_{tr}L}}, & M(\xi) = \sum M_{tr}\dfrac{\mathscr{T}_t(\gamma_{tr}\xi)}{\sqrt{\zeta_{tr}L}} \\ r \in N \quad t \in \{0,1\} & r \in N \quad t \in \{0,1\} \end{cases} \tag{10b}$$

By expressing the generalized displacements $w(\xi)$, $\psi(\xi)$ in terms of the MFs of Eq. (10a), considering the properties of the MFs of Eq. (3), and combining Eqs. (8)–(10), we can arrive at

$$\begin{pmatrix} Q(\xi) \\ M(\xi) \end{pmatrix} = \sum \begin{pmatrix} d_{11;ls} & d_{12;ls} \\ d_{21;ls} & d_{22;ls} \end{pmatrix} \begin{pmatrix} w_{ls}\dfrac{\mathscr{T}_l(\gamma_{ls}\xi)}{\sqrt{\zeta_{ls}L}} \\ \psi_{ls}\dfrac{\mathscr{T}_l(\gamma_{ls}\xi)}{\sqrt{\zeta_{ls}L}} \end{pmatrix} \quad \begin{matrix} s \in N \\ l \in \{0,1\} \end{matrix} \tag{11}$$

in which

$$\begin{aligned} d_{11;ls} &= EI_1\gamma_{ls}^4 + T\gamma_{ls}^2 - \rho A\omega^2 \\ d_{12;ls} &= d_{21;ls} = -EI_{12}c_0\gamma_{ls}^4 + Tc_2\gamma_{ls}^2 - \rho Ac_2\omega^2 \\ d_{22;ls} &= \left(E\Gamma + EI_2c_0^2\right)\gamma_{ls}^4 + GJ\gamma_{ls}^2 + T\left(c_1^2 + c_2^2\right)\gamma_{ls}^2 - \left[I + \rho A\left(c_1^2 + c_2^2\right)\right]\omega^2 \end{aligned} \tag{12}$$

Next, expanding both sides of Eq. (11) by using the modified Fourier series as in Eq. (10b), we have

$$\begin{cases} Q_{tr} = \displaystyle\int_{-L}^{L} \sum \left[\left(d_{11;ls}w_{ls} + d_{12;ls}\psi_{ls}\right)\frac{\mathscr{T}_l(\gamma_{ls}\xi)}{\sqrt{\zeta_{ls}L}}\right]\frac{\mathscr{T}_t(\gamma_{tr}\xi)}{\sqrt{\zeta_{tr}L}}d\xi & \begin{matrix} s \in N \\ l \in \{0,1\} \end{matrix} \\ M_{tr} = \displaystyle\int_{-L}^{L} \sum \left[\left(d_{21;ls}w_{ls} + d_{22;ls}\psi_{ls}\right)\frac{\mathscr{T}_l(\gamma_{ls}\xi)}{\sqrt{\zeta_{ls}L}}\right]\frac{\mathscr{T}_t(\gamma_{tr}\xi)}{\sqrt{\zeta_{tr}L}}d\xi & \begin{matrix} s \in N \\ l \in \{0,1\} \end{matrix} \end{cases} \tag{13}$$

Eq. (13) illustrates the relationship between the modified Fourier series coefficients of force and displacement of the beam stiffener which can be expressed in the following matrix form

$$\boldsymbol{f}^b = \begin{pmatrix} \boldsymbol{Q}^b \\ \boldsymbol{M}^b \end{pmatrix} = \begin{pmatrix} \boldsymbol{K}_{11}^b & \boldsymbol{K}_{12}^b \\ \boldsymbol{K}_{21}^b & \boldsymbol{K}_{22}^b \end{pmatrix} \begin{pmatrix} \boldsymbol{w}^b \\ \boldsymbol{\psi}^b \end{pmatrix} = \boldsymbol{K}^b\boldsymbol{d} \tag{14}$$

where $\boldsymbol{K}^b$ is the SDS matrix of the beam stiffener. The concise analytical expression of the each sub-matrix $\boldsymbol{K}_{ij}^b$ of the SDS matrix can be written in the form of 2×2 block matrix as

$$\boldsymbol{K}_{ij}^b = \begin{bmatrix} \boldsymbol{K}_{ij;00}^b & \boldsymbol{K}_{ij;01}^b \\ \boldsymbol{K}_{ij;10}^b & \boldsymbol{K}_{ij;11}^b \end{bmatrix} \quad i,j \in \{1,2\} \tag{15}$$

The concise analytical expression of $\boldsymbol{K}_{ij;lt}^b$ is as follows,

$$\boldsymbol{K}_{ij;lt}^b(s,r) = \frac{1}{\sqrt{\zeta_{ls}\zeta_{tr}}L}\int_{-L}^{L} d_{ij;ls}\mathscr{T}_l(\gamma_{ls}\xi)\mathscr{T}_t(\gamma_{tr}\xi)\mathrm{d}\xi \quad l,t \in \{0,1\}; s,r \in N \tag{16}$$

which leads to analytical expressions for $\boldsymbol{K}_{ij;lt}^b$ once the analytical ex-

pressions for the functions of cross section parameters (such as $EI_1(x)$, $\rho A(x)$, $EI_{12}(x)$.etc.) of $d_{ij;ls}$ in Eq. (12) of the beam stiffener in frequency domain are provided. It should be mentioned in passing that in $\boldsymbol{K}^b_{ij;lt}$, l and t take either 0 or 1 while s and r take 0,1, …,N-1, therefore the matrix size of $\boldsymbol{K}^b_{ij;lt}$ is $2N\times 2N$. In particular, if $d_{ij;ls}$ is a constant with respect to x, then from Eq. (16) we know that $\boldsymbol{K}^b_{ij;lt}$ becomes a $2N\times 2N$ identity matrix multiplied by the constant $d_{ij;ls}$.

So far we have provided the SDS formulation of an open-section beam stiffener. The formulation considers the warpage of the open-section beam, the eccentricity of the centroid (mass axis), shear center (elastic axis), as well as the connection point. In essence, there are a wide range of beam-stiffened plates can be modelled by the model discussed above, which provides a wide practical application scope.

2.2.2. SDSM of beam stiffeners with different closed-sections

Next, the SDS matrices of several closed-section beams will be developed following similar procedure as in Section 2.2.1, to expand its applicability range.

As shown in Fig. 2, a closed-section beam connected to the plate along the projection of the beam's centre line where point P is located on its bottom surface, and the centre point coincides with the shear centre. As shown in Fig. 3, another closed-section beam connected to the plate where the beam's centre line, connecting line and shear coincide with each other. In the above two different beam sections, point C is the centroid of the section, c_1 and c_2 are the offsets of points C and P in the z and x directions, w is the displacement of the point P in the z direction, parameters H and Q are the forces applied to the point P in the x and z directions respectively, and M is the torsional moment. The stretching of the structure caused by the bending motion, and the warping effect due to the closed section can be ignored. Therefore, based on the classical beam theory, the vibration of the beam stiffener can be expressed as

$$\begin{cases} \dfrac{\partial^2}{\partial y^2}\left(EI_1\dfrac{\partial^2 w_r}{\partial y^2}\right) - m_r\omega^2 w - m_r\omega^2 c_2\psi = Q \\ GJ\dfrac{\partial^2\psi}{\partial y^2} + \left[I + m_r\left(c_1^2+c_2^2\right)\right]\omega^2\psi - m_r\omega^2 c_2 w = M \end{cases} \tag{17}$$

where I_1 is the main moment of inertia of the beam section on the x axis. E is the elastic modulus of the material, m_r is the mass per unit length of the beam, G and J are the shear modulus of the material and the mass moment of inertia with respect to the shear center respectively, and I is the torsional section factor. Following similar procedure as in Section 2.2.1, the following equations can be derived from Eq. (17)

$$\begin{cases} \left(EI_1k_n^4 - m_r\omega^2\right)w - m_r\omega^2 c_2\psi = Q \\ \left[-GJk_n^2 + \left[I + m_r\left(c_1^2+c_2^2\right)\right]\omega^2\right]\psi - m_r\omega^2 c_2 w = M \end{cases} \tag{18}$$

The above equations can be rewritten in the following matrix form

$$\begin{pmatrix} Q(\xi) \\ M(\xi) \end{pmatrix} = \sum \begin{pmatrix} d_{11;ls} & d_{12;ls} \\ d_{21;ls} & d_{22;ls} \end{pmatrix} \begin{pmatrix} w_{ls}\dfrac{\mathscr{T}_l(\gamma_{ls}\xi)}{\sqrt{\zeta_{ls}L}} \\ \psi_{ls}\dfrac{\mathscr{T}_l(\gamma_{ls}\xi)}{\sqrt{\zeta_{ls}L}} \end{pmatrix} \quad \begin{matrix} s\in N \\ l\in\{0,1\} \end{matrix}$$

When the cross-sectional shape of the beam is as shown in Fig. 2, $c_2 = 0$. It can be obtained according to Eq. (12),

$$\begin{aligned} d_{11;ls} &= EI_1{\gamma_{ls}}^4 - m_r\omega^2 \\ d_{12;ls} &= d_{21;ls} = 0 \\ d_{22;ls} &= -GJ{\gamma_{ls}}^2 + \left(I + m_r c_1^2\right)\omega^2 \end{aligned} \tag{19}$$

When the cross-sectional shape of the beam is as shown in Fig. 3, $c_1 = 0$.So the parameters in Eq. (12) can be simplified to

$$\begin{aligned} d_{11;ls} &= EI_1{\gamma_{ls}}^4 - m_r\omega^2 \\ d_{12;ls} &= d_{21;ls} = -m_r\omega^2 c_2 \\ d_{22;ls} &= -GJ{\gamma_{ls}}^2 + \left(I + m_r c_2^2\right)\omega^2 \end{aligned} \tag{20}$$

So far, the SDS formulation of two types of closed-section beam stiffeners have been developed.

2.3. Assembly procedure of global spectral dynamic stiffness matrix

Now we can assemble the SDS matrices of both plates and beam stiffeners. To explain the assembly process in a simple manner, but without loss of generality, we adopt the example shown in Fig. 4, in which a plate structure is connected to a beam along the beam's bottom center line along the first line nodes $(\boldsymbol{w}_p^{(1)}, \boldsymbol{\psi}_p^{(1)})$ (Notice that the plate has 8 line nodes and the beam has 2 line nodes). Superimposing the beam SDS matrix $\boldsymbol{K}_b$ in Eq. (14) to the rows and columns corresponding to the first and second line nodes of the plate SDS matrix $\boldsymbol{K}_p$ like Fig. 5. If a beam stiffer is superimposed onto the ith and $(i+1)$th line nodes of a plate, the overall SDS matrix can be assembled from the SDS matrices of both the plate and the beam stiffener as given in Eq. (21) and illustrated in Fig. 5.

It is worth noting that the materials properties of both the beam stiffener and the plate can be either frequency independent or frequency dependent (such as honeycomb sandwich panels [52–55]). It is due to the SDS matrices are in frequency domain which can model both situations.

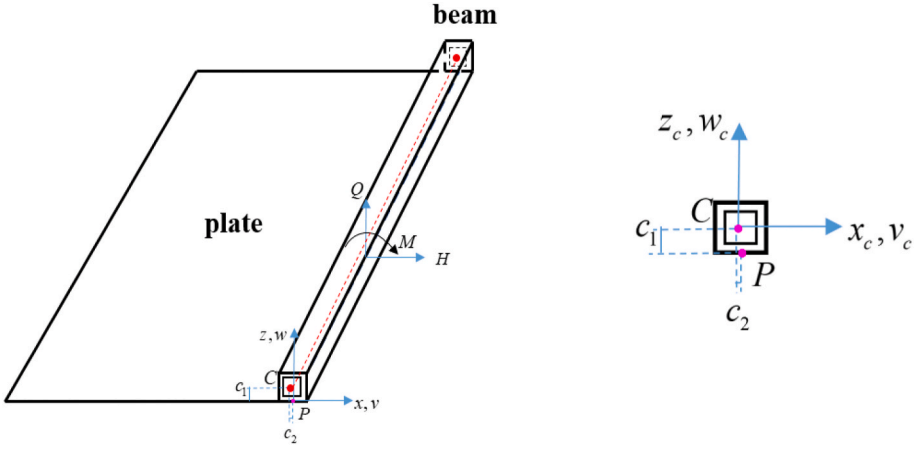

Fig. 2. A closed-section beam stiffened plate with eccentricity.

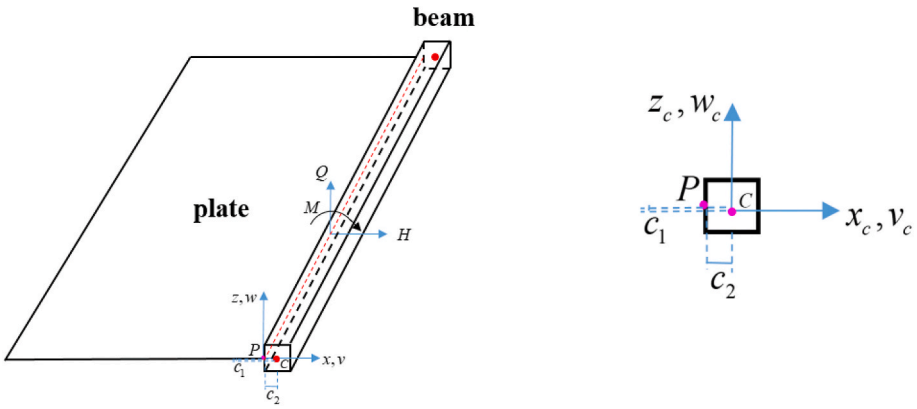

Fig. 3. A closed-section beam stiffened plate without eccentricity.

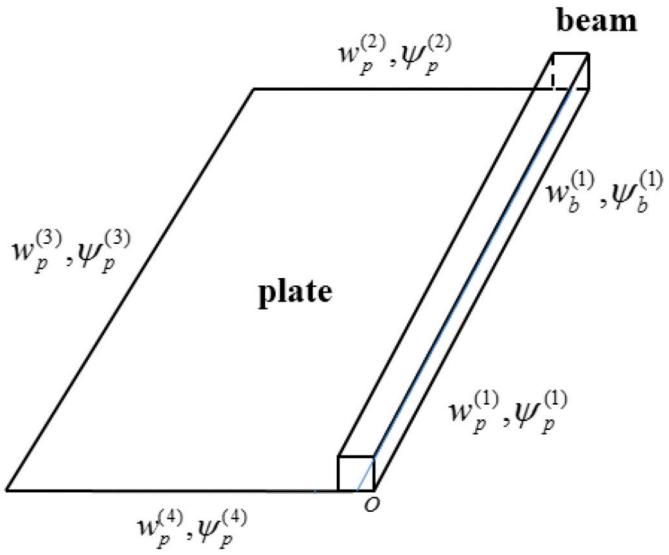

Fig. 4. Line nodes of a closed-section-beam stiffened plate.

2.4. Applying boundary conditions and Wittrick-Williams algorithm for modal analysis

In proposed method described above, any prescribed boundary conditions can be applied following similar procedure generally used in the finite element method. For the assembly procedure and application of boundary conditions to arrive at the solution of the final SDS matrix of the structure, interested readers are referred to Refs. [30,42].

The algorithm of Wittrick and Williams (WW) with the so-called *J0* count problem resolved properly can be applied to compute the natural frequencies. (Bandgap analysis [56–58] of periodic beam-stiffened plates can also be performed by using extended WW algorithm [59]). The procedure is described in detail in Refs. [26,29]. It is worth noting that since the DOFs of beam stiffeners in the form of spectra (i.e. coefficient of modified Fourier series) are superposed directly to those of the plate element boundaries, where no extra DOFs has been introduced in the SDS formulation. It is therefore understandable that the *J0* count of beam is not needed to be added to the *J0* count of the plate. That is to say, only the *J0* count from the plate elements are required for the WW algorithm for modal analysis for the beam stiffened plate.

The complete procedure of the dynamic stiffness development and its implementation are illustrated in Fig. 6.

$$\begin{bmatrix} \boldsymbol{K}^p_{11}+\boldsymbol{K}^b_{11} & \boldsymbol{K}^p_{12}+\boldsymbol{K}^b_{12} & \boldsymbol{K}^p_{13} & \boldsymbol{K}^p_{14} & \boldsymbol{K}^p_{15} & \boldsymbol{K}^p_{16} & \boldsymbol{K}^p_{17} & \boldsymbol{K}^p_{18} \\ \boldsymbol{K}^p_{21}+\boldsymbol{K}^b_{21} & \boldsymbol{K}^p_{22}+\boldsymbol{K}^b_{22} & \boldsymbol{K}^p_{23} & \boldsymbol{K}^p_{24} & \boldsymbol{K}^p_{25} & \boldsymbol{K}^p_{26} & \boldsymbol{K}^p_{27} & \boldsymbol{K}^p_{28} \\ \boldsymbol{K}^p_{31} & \boldsymbol{K}^p_{32} & \boldsymbol{K}^p_{33} & \boldsymbol{K}^p_{34} & \boldsymbol{K}^p_{35} & \boldsymbol{K}^p_{36} & \boldsymbol{K}^p_{37} & \boldsymbol{K}^p_{38} \\ \boldsymbol{K}^p_{41} & \boldsymbol{K}^p_{42} & \boldsymbol{K}^p_{43} & \boldsymbol{K}^p_{44} & \boldsymbol{K}^p_{45} & \boldsymbol{K}^p_{46} & \boldsymbol{K}^p_{47} & \boldsymbol{K}^p_{48} \\ \boldsymbol{K}^p_{51} & \boldsymbol{K}^p_{52} & \boldsymbol{K}^p_{53} & \boldsymbol{K}^p_{54} & \boldsymbol{K}^p_{55} & \boldsymbol{K}^p_{56} & \boldsymbol{K}^p_{57} & \boldsymbol{K}^p_{58} \\ \boldsymbol{K}^p_{61} & \boldsymbol{K}^p_{62} & \boldsymbol{K}^p_{63} & \boldsymbol{K}^p_{64} & \boldsymbol{K}^p_{65} & \boldsymbol{K}^p_{66} & \boldsymbol{K}^p_{67} & \boldsymbol{K}^p_{68} \\ \boldsymbol{K}^p_{71} & \boldsymbol{K}^p_{72} & \boldsymbol{K}^p_{73} & \boldsymbol{K}^p_{74} & \boldsymbol{K}^p_{75} & \boldsymbol{K}^p_{76} & \boldsymbol{K}^p_{77} & \boldsymbol{K}^p_{78} \\ \boldsymbol{K}^p_{81} & \boldsymbol{K}^p_{82} & \boldsymbol{K}^p_{83} & \boldsymbol{K}^p_{84} & \boldsymbol{K}^p_{85} & \boldsymbol{K}^p_{86} & \boldsymbol{K}^p_{87} & \boldsymbol{K}^p_{88} \end{bmatrix}$$

Fig. 5. Assembly procedure of the overall SDS matrixes of a plate stiffened by a beam stiffener.

$$\begin{aligned} \boldsymbol{K}_{i,i} &= \boldsymbol{K}^p_{i,i} + \boldsymbol{K}^b_{11}, \quad \boldsymbol{K}_{i,i+1} = \boldsymbol{K}^p_{i,i+1} + \boldsymbol{K}^b_{12} \\ \boldsymbol{K}_{i+1,i} &= \boldsymbol{K}^p_{i+1,i} + \boldsymbol{K}^b_{21}, \quad \boldsymbol{K}_{i+1,i+1} = \boldsymbol{K}^p_{i+1,i+1} + \boldsymbol{K}^b_{22} \end{aligned} \tag{21}$$

3. Numerical examples

In order to verify the accuracy and efficiency of the proposed SDSM for beam stiffened plates, we adopt several beam-stiffened-plate models and perform numerical analysis based on MATLAB code. We also take a rigorous recourse to finite element models by using the software ANSYS, for a direct comparison of results. The natural frequencies and mode shapes computed by our theory and those computed using ANSYS are critically examined. To demonstrate the versatility of our method, we use different plate structures stiffened by different stiffeners and with different boundary conditions as illustrations.

Unless otherwise specified, in all example models, the size of the rectangular plate is $2a \times 2b$, in which $2a = 2b = 1m$, thickness: $h = 5mm$.The material properties of the plate and the beam are as follows: Young's modulus $E_1 = 7.1 \times 10^{10} Pa$, Poisson's ratio $\nu = 0.3$, density $\rho_1 = 2660 kg/m^3$. All the computations in this paper are performed on the same computer with an AMD A6-3420 M CPU with 6GB RAM. For

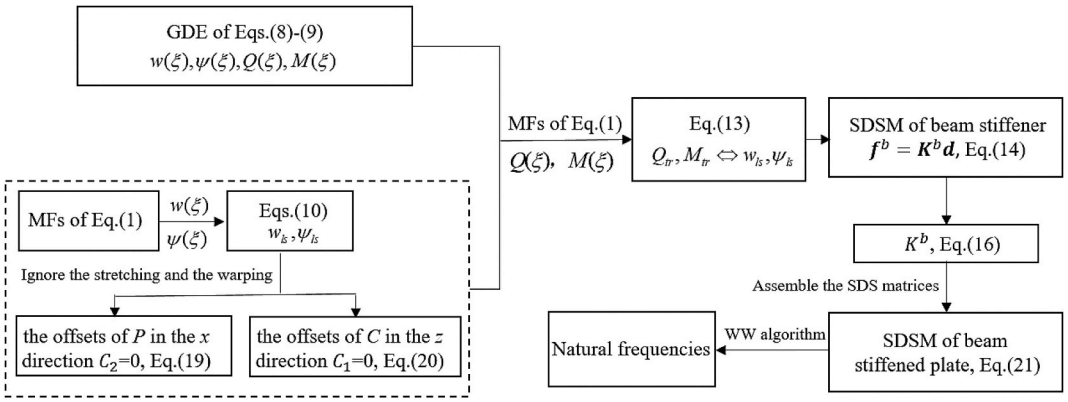

Fig. 6. Flowchart showing the procedure for the DSM development and its implementation.

the plate boundary conditions, clamped or built-in support is represented by C, simple support is represented by S, and free or supportless is represented by F.

3.1. Example 1: closed-section beam stiffened plates

In this section, the natural frequencies of the closed-section beam stiffened plates are computed to verify the accuracy of the SDSM. Fig. 7 (a) shows the finite element model of a plate stiffened by closed-section beam without eccentricity, where the four sides of the plate are completely free. In the finite element model, the general shell element and beam element are selected as the element type of the structure based on the classic thin plate theory and beam theory. The length of the beam is $1m$, and the cross-section size is $0.05m \times 0.05m$. Fig. 7(b) is the numbering of the four sides of the structure to indicate the boundary conditions (for example, from 1 to 4 sides are 'S', 'G', 'F' and 'C', then it is denoted as SGFC).

Table 1 shows the natural frequencies of an SFFF plate stiffened by non-eccentric closed-section beams (Fig. 7) with different FE mesh size and Fourier series of the SDSM. It can be seen that the DSM results converge up to the fifth significant figures or digits when N is 20; the DOFs adopted in the DSM is only 280 of that in the FEM; the computational time for the DSM is less than 1% of that by the FEM ($0.003m \times 0.003m$) yet the FEM results have only four significant digit accuracy. Under the premise of ensuring representativeness, in all subsequent examples, the FE mesh size is set to $0.003m \times 0.003m$ and SDSM uses 25 Fourier series in all cases.

Next, we revisit two cases previously studied in Ref. [4] by using the current method. It is a plate with one edge stiffened for varying values of stiffener's depth. The size of the square plate is $a \times a$, thickness: $h_p = 0.04$in.. The material properties of the plate and the stiffener are as follows: Young's modulus $E_4 = 10.5 \times 10^6 \text{lb/in}^2$, density $\rho_4 = 0.101\text{lb sec}^2/\text{in}^4$, Poisson's ratio $\nu = 0.3$. The dimensions of the stiffeners were related to stiffener depth. I-beam horizontal size at both ends $b_4 = h_4/2$, thin-wall thickness $t_w = t_f = h_4/25$. The nondimensional frequency parameter $\lambda = \omega^2 a\sqrt{\rho_4/D}$. D is the flexural rigidity. Tables 1 and 2 in Ref. [4] the results of computation for the lowest frequency coefficient are presented. Table 1 in Ref. [4] is associated with S–S–S–F plates. Table 2 in Ref. [4] is associated with S–C–S–F plates. The edge with F boundary condition is stiffened.

In Table 2, we used SDSM to calculate the first few eigenvalues of the two cases, it can be seen that all the values agree very well with those in Ref. [4].

Table 3 shows the representative natural frequencies of a beam stiffened plate with eight different sets of boundary conditions. Fig. 8 shows some representative mode shapes of a stiffened plate with SFCF boundary conditions.

Table 1 shows the convergence of SDSM and FEM for SFFF, Table 2 is in agreement with the results of Ref. [4], and it can be seen from Table 3 that the results from SDSM and FEM with various boundary conditions are very close to each other. (The small difference indicates a good consistency between the two methods.) It can also be ascertained from Fig. 8 that the modes computed from the two methods match very well. Clearly, the accuracy of the SDSM is verified. It should be noted that the SDSM has taken only 25 Fourier series to compute the modes, and the calculation speed is quite impressive. On the question of accuracy, the SDSM has significant advantage when compared with the finite element solution which requires much finer mesh.

3.2. Example 2: An L-cross-section beam stiffened plate

In this section, the L-cross-section beam stiffened plates is used to

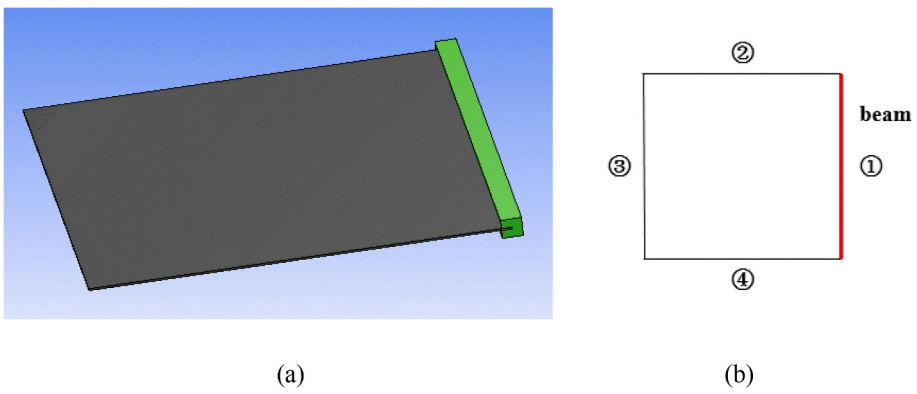

Fig. 7. The FE model of a plate stiffened by closed-section beam without eccentricity and the numbering of the plate boundaries.

Table 1
Natural frequencies (Hz) of an SFFF plate stiffened by non-eccentric closed-section ($0.05m \times 0.05m$) beams (Fig. 7) with different FE mesh size and Fourier series of the SDSM.

Mode	SDSM				FEM			
	$N = 10$	$N = 15$	$N = 20$	$N = 25$	$0.005m \times 0.005m$	$0.004m \times 0.004m$	$0.003m \times 0.003m$	$0.002m \times 0.002m$
Time(s)	1.76	2.29	3.42	4.83	87	161	579	9854
DOFs	140	210	280	350	243,627	380,337	670,794	1509006
1	10.537	10.538	10.539	10.539	10.529	10.528	10.527	10.526
2	18.572	18.572	18.572	18.572	18.569	18.569	18.569	18.569
3	33.370	33.370	33.371	33.371	33.347	33.345	33.342	33.341
4	38.314	38.317	38.320	38.320	38.283	38.278	38.274	38.272
5	60.849	60.849	60.849	60.849	60.837	60.834	60.831	60.830
6	67.561	67.563	67.566	67.566	67.467	67.456	67.447	67.442

Table 2
The comparison results of the SDSM with the data of Tables 1 and 2 in Ref. [4].

Mode (λ)	$h_4 = 0$				$h_4 = 0.3$			
	Table 1 in Ref. [4]		Table 2 in Ref. [4]		Table 1 in Ref. [4]		Table 2 in Ref. [4]	
	SDSM	Ref. [4]	SDSM	Ref [.4]	SDSM	Ref [.4]	SDSM	Ref [.4]
1	11.5622	11.6845	19.3427	19.5098	12.5732	12.6874	23.0132	23.1040
2	27.4648	–	49.2071	–	33.0124	–	51.1325	–
3	41.0322	–	49.3021	–	41.4378	–	58.2113	–
4	59.0165	–	78.0213	–	63.0153	–	85.8932	–
5	61.4213	–	98.2154	–	72.1075	–	99.8523	–

Table 3
Representative natural frequencies (Hz) of a beam stiffened plate with eight sets of boundary conditions.

BC	Mode	SDSM	FEM
SFCF	1st	18.87	18.87
SSCF	5th	94.93	94.83
FCCC	4th	134.28	134.32
FSSS	2nd	64.19	64.09
FCSC	3rd	88.37	88.34
FFFF	3rd	33.45	33.39
SSSS	7th	165.95	165.65
SCSC	6th	162.08	162.05

further investigate the effect of the beam stiffeners on the plate vibration and to verify the accuracy of the method. As shown in Fig. 9(a), it is a finite element model of an L-cross-section-beam stiffened plate. The cross-sectional dimensions are shown in Fig. 9(b), where $c_0 = 0.035m$, $c_1 = 0.027m$, $c_2 = 0.077m$, and the remaining parameters are the same as Example 1. Table 4 shows the natural frequencies of a beam stiffened plate with four sets of boundary conditions. Fig. 10 shows some representative mode shapes by SDSM and FEM for the SFFF plate.

It can be seen from Table 4 that when the structure is essentially L-cross-section beam stiffened plates, there are little discrepancies in the natural frequencies between the SDSM and the FEM. Also, Fig. 10 indicates that the two sets of mode shapes match well.

3.3. Example 3: A T-beam stiffened plate

In this section, an example with a T-beam stiffened plate is analyzed. The structure is shown in Fig. 11(a). Side by side to the application of the current SDSM theory, a finite element model of this structure is also created. The cross-sectional dimensions are shown in Fig. 11(b), and the remaining parameters are the same as Example 1. Fig. 12 gives the boundary conditions of the structure. Table 5 shows the comparison of the natural frequencies of 1st to 6th modes obtained by the SDSM and the finite element model under different cross-sectional area. Fig. 13

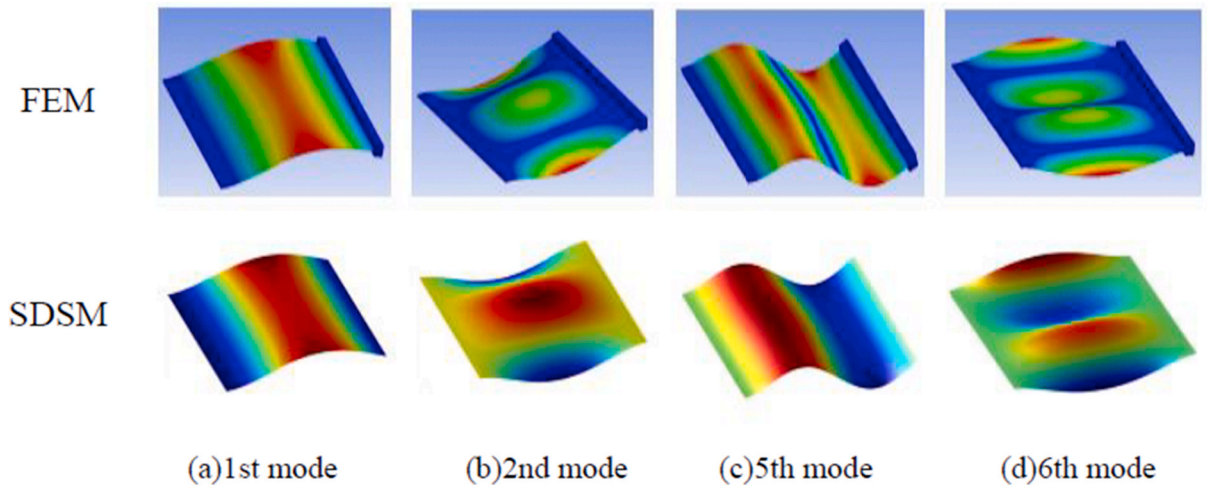

Fig. 8. Mode shapes by FEM and SDSM for a stiffened plate subject to SFCF boundary conditions.

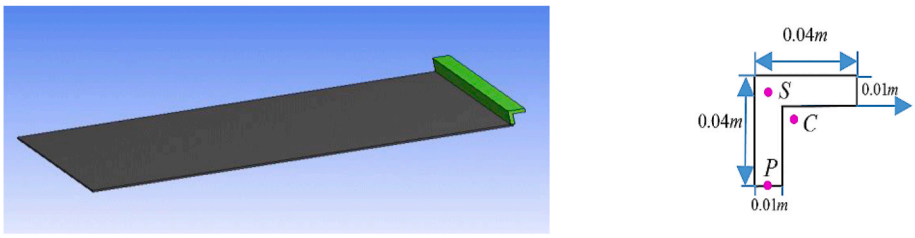

Fig. 9. The finite element model of a plate stiffened by L-cross-section beam.

Table 4
The natural frequencies (*Hz*) of a beam stiffened plate in Fig. 9 with four different BCs.

Mode	SFCF		SFFF		FSFS		SSCF	
	SDSM	FEM	SDSM	FEM	SDSM	FEM	SDSM	FEM
1	18.88	18.87	9.67	9.64	15.07	15.07	22.58	22.41
2	29.38	29.31	18.57	18.57	36.60	36.73	42.37	42.19
3	53.28	53.14	33.20	33.15	51.68	51.67	65.49	65.21
4	61.14	61.06	35.05	34.96	76.59	76.69	82.42	82.32
5	75.45	75.31	60.98	60.91	78.42	79.27	91.12	90.69
6	98.99	98.86	66.51	66.31	112.64	112.59	131.49	130.93

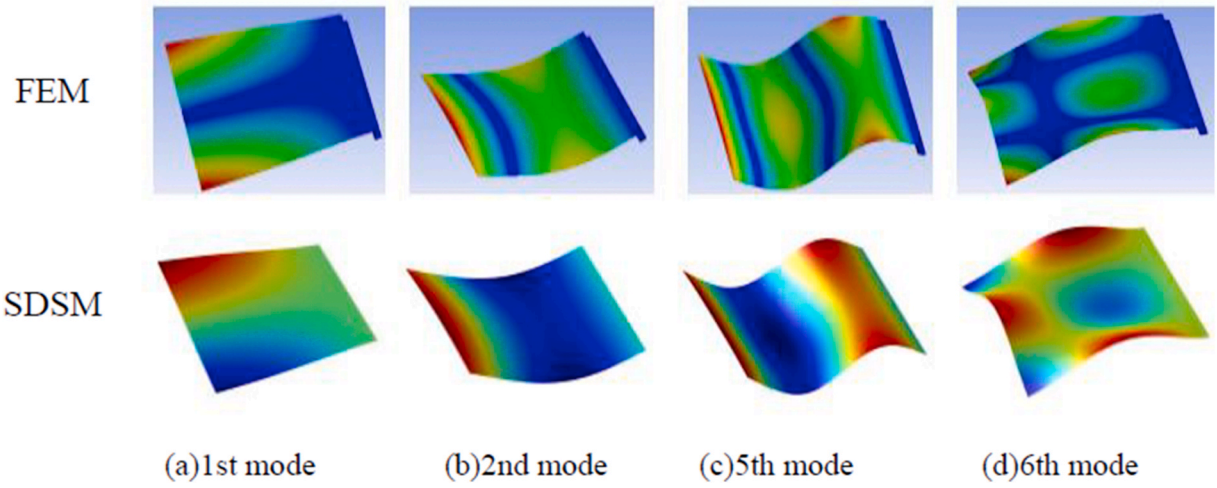

Fig. 10. Mode shapes of a beam stiffened SFFF plate in Fig. 9 by FEM and SDSM.

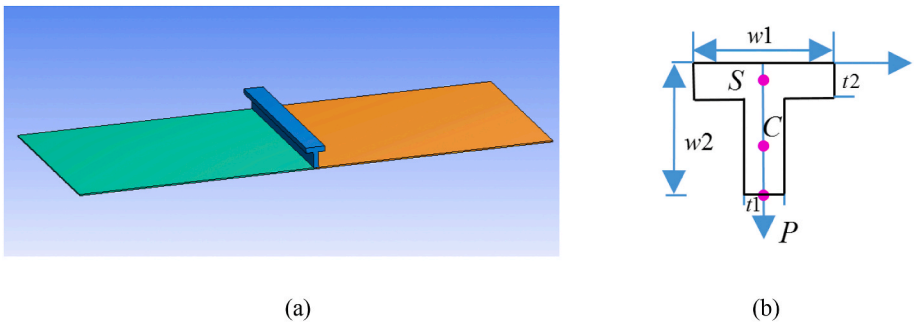

Fig. 11. The finite element model of a T-beam stiffened plate.

compares some representative mode shapes of a T-beam stiffened plate whose stiffener is of cross-section: $t_1 = t_2 = 0.02m$, $w_1 = w_2 = 0.08m$.

It can be seen from Table 5 that the results of both the SDSM and the finite element method are in good agreement for a T-beam stiffened plate with stiffeners of different cross-sections. Fig. 13 shows the 1st, 3rd, 5th and 6th mode shapes of a stiffened plate where the T-shaped stiffener's cross-section is $t_1 = t_2 = 0.02m$, $w_1 = w_2 = 0.08m$ by using both the FEM and the SDSM. It is obvious that the mode shapes

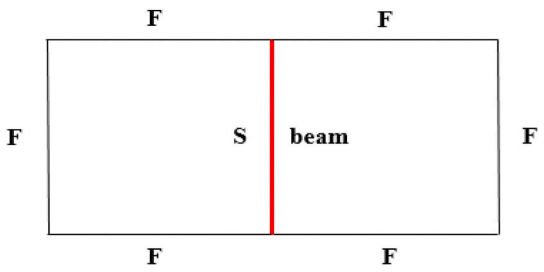

Fig. 12. The boundary conditions of the T-beam stiffened plate.

computed by both methods agree very well.

3.4. Example 4: complex beam stiffened plates

In this section, two complex beam stiffened plates structures are selected to further verify the accuracy and versatility.

The first example as show in Fig. 14 is a rectangular plate stiffened by two stiffeners with cross-sections given therein, and the structure is subjected to the boundary conditions depicted in Fig. 15. For simplicity, the remaining parameters are the same as Example 1. Table 6 compares the natural frequencies computed by both the SDSM and the FEM and Fig. 16 gives the comparisons of some representative mode shapes.

It can be seen from Table 6 that for the structure depicted in Fig. 14, the results of SDSM and FEM agree very well. At the same time, the mode shapes computed from two methods shown in Fig. 16 match well.

The second example as show in Fig. 17(a) is an L-shaped plate stiffened by three beam stiffeners, and the structure is subjected to the boundary conditions depicted in Fig. 17(b). For simplicity, the remaining parameters are the same as Example 1. Table 7 compares the natural frequencies by both SDSM and FEM and Fig. 18 shows some representative mode shapes.

It can be seen from Table 7 and Fig. 18 that both the natural frequencies and mode shapes of the stiffened L-shaped plate by using both the FEM and the SDSM match well with each other. This example further proves that the SDSM is an accurate and versatile tool for the dynamic analysis of complex beam-stiffened plates.

4. Conclusions

A novel spectral dynamic stiffness (SDS) theory has been proposed for plate structures stiffened by beam stiffeners with either open or close sections and with or without eccentricity. According to the relationship between the forces and the displacements at the common edge of the plate edges and the beam stiffener, the vibrational equation of the stiffeners with both open section and closed section are formulated

Table 5
Natural frequencies (*Hz*) of the plate structure in Fig. 11 stiffened by beams with different cross-sections.

Mode	$t_1 = t_2 = 0.01m$ $w_1 = w_2 = 0.04m$		$t_1 = t_2 = 0.015m$ $w_1 = w_2 = 0.06m$		$t_1 = t_2 = 0.02m$ $w_1 = w_2 = 0.08m$		$t_1 = t_2 = 0.025m$ $w_1 = w_2 = 0.1m$	
	SDSM	FEM	SDSM	FEM	SDSM	FEM	SDSM	FEM
1	4.32	4.32	4.32	4.32	4.32	4.32	4.32	4.32
2	9.27	9.28	10.13	10.11	10.44	10.41	10.51	10.50
3	10.58	10.57	10.58	10.57	10.58	10.57	10.58	10.57
4	18.59	18.58	18.54	18.53	18.36	18.33	18.29	17.93
5	26.48	26.47	26.48	26.47	26.48	26.47	26.48	26.47
6	33.04	33.01	33.30	33.26	33.34	33.31	33.34	33.28

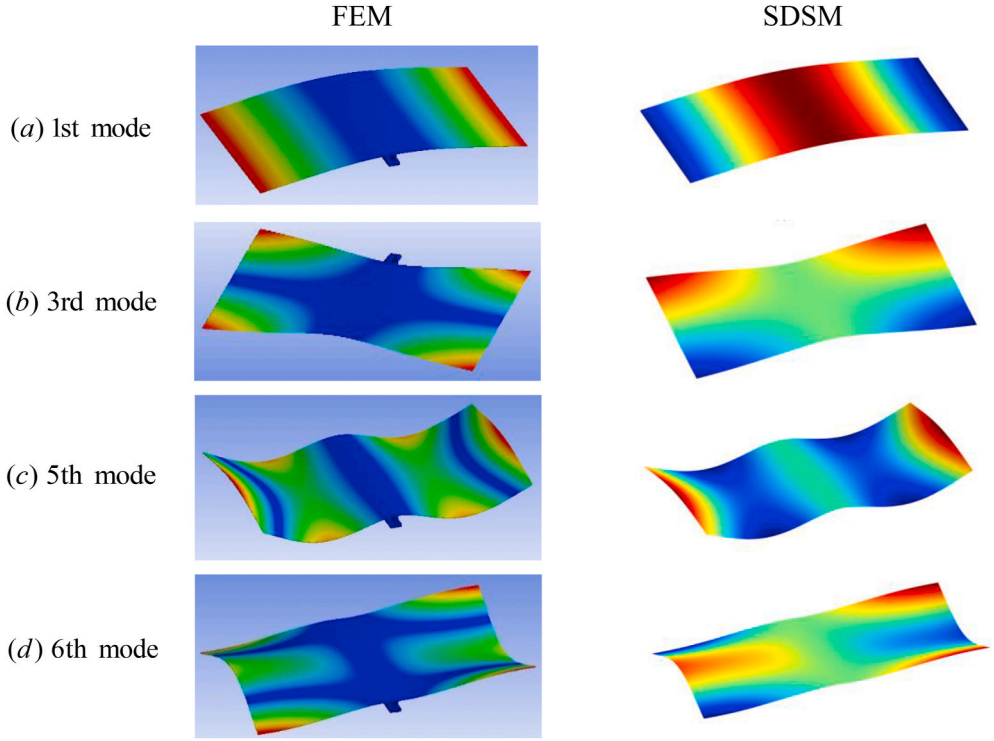

Fig. 13. Mode shapes for a T-beam stiffened plate in Fig. 11 with $t_1 = t_2 = 0.02m$ and $w_1 = w_2 = 0.08m$ by using FEM and SDSM.

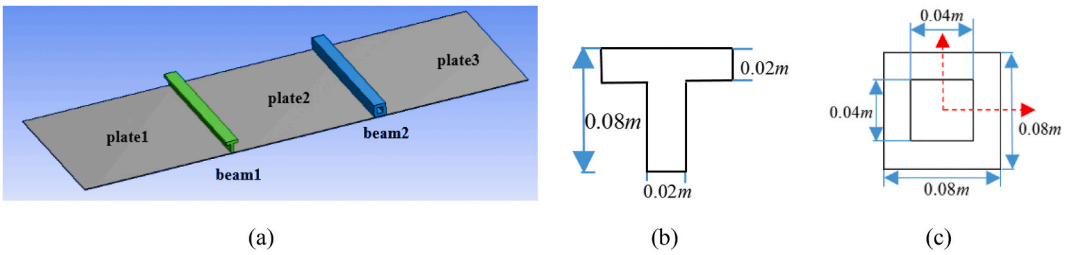

Fig. 14. A rectangular plate stiffened by two stiffeners with different cross-sections.

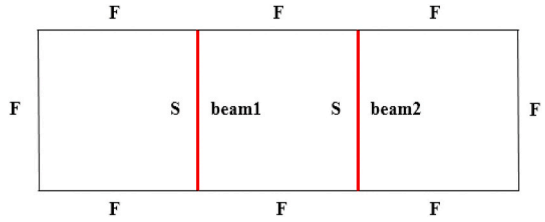

Fig. 15. The boundary conditions of the two-beam stiffened plate in Fig. 14.

based on modified Fourier series. The SDS matrices of beam stiffeners with the inclusion of warping stiffness have been developed. The ensuing SDS matrices of beam stiffeners are superposed directly onto the overall SDS matrix of the plate assemblies to model the beam-stiffened plate structure accurately. By using the Wittrick-Williams algorithm, the natural frequencies and mode shapes are extracted. A wide ranging and well-thought-out number of examples are given to illustrate the versatility and accuracy of the proposed method. The research has broadened the scopes of recently proposed SDS theories for plate assemblies to a higher level by accounting for beam-stiffeners of complex cross-sections connected to the plate assemblies. The research carried out in this paper is of great significance when analysing stiffened plate structures which have applications in the transport [60], aeronautical, ship-building industries, amongst others.

Author statement

Xiang Liu: Conceptualization, Methodology, Writing – review & editing, Supervision, Investigation, Project administration, Funding acquisition. Yu Li: Investigation, Data curation, Writing – original draft preparation, Writing- Reviewing and Editing Yuliang Lin: Writing-

Table 6
Natural frequencies of a two-beam stiffened plate in Fig. 14

Mode(*Hz*)	1	2	3	4	5	6	7	8
SDSM	2.44	3.34	10.51	10.58	15.32	21.81	26.84	32.50
FEM	2.44	3.34	10.49	10.56	15.26	21.75	26.83	32.42

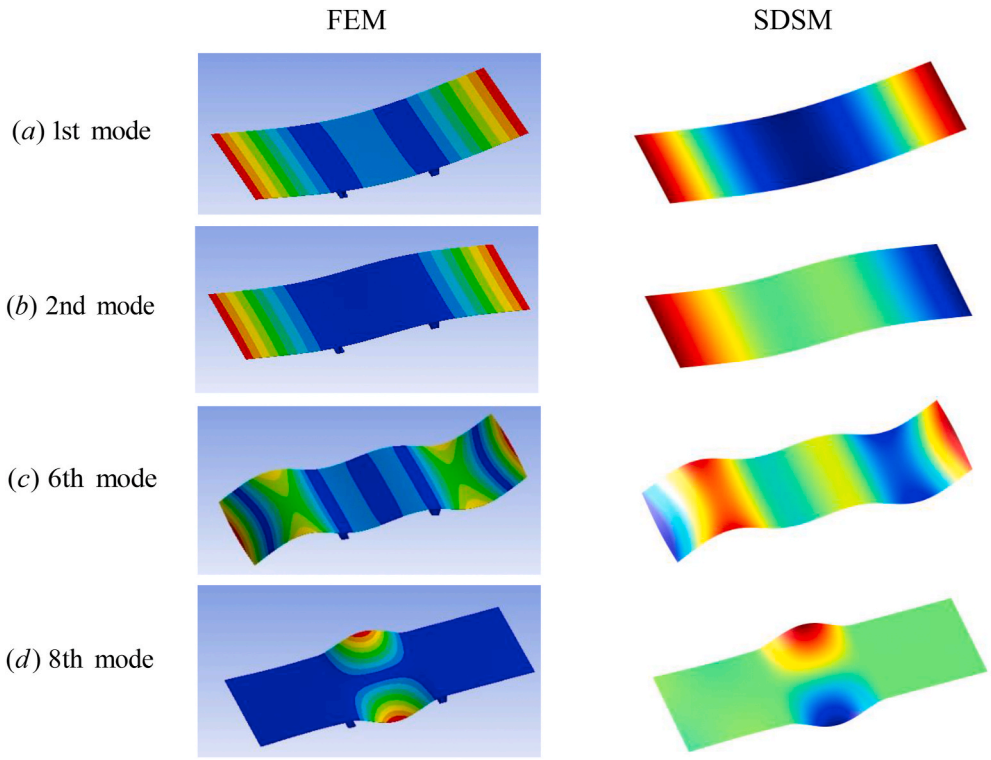

Fig. 16. Mode shapes of a two-beam-stiffened plate in Fig. 14 by FEM and SDSM.

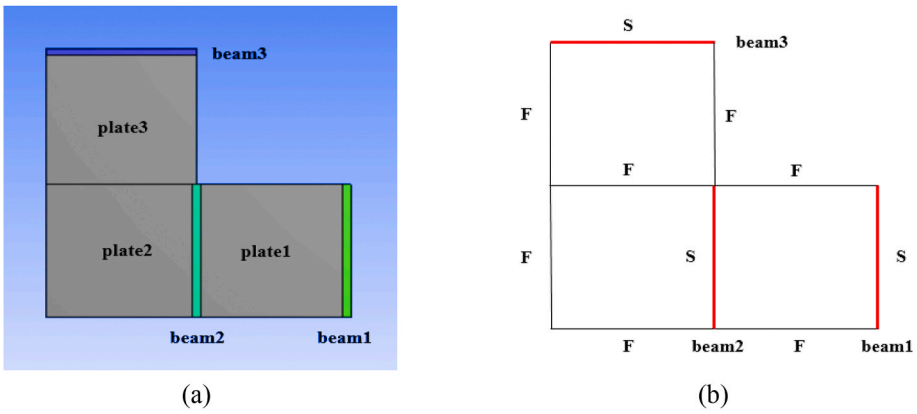

Fig. 17. An L-shaped plate stiffened by three beam stiffeners and the boundary conditions.

Table 7
Natural frequencies of the stiffened L-shaped plate in Fig. 17

Mode(*Hz*)	1	2	3	4	5	6	7	8
SDSM	3.55	9.08	14.59	17.24	24.27	26.67	32.49	35.88
FEM	3.55	9.09	14.58	17.24	24.27	26.68	32.47	35.87

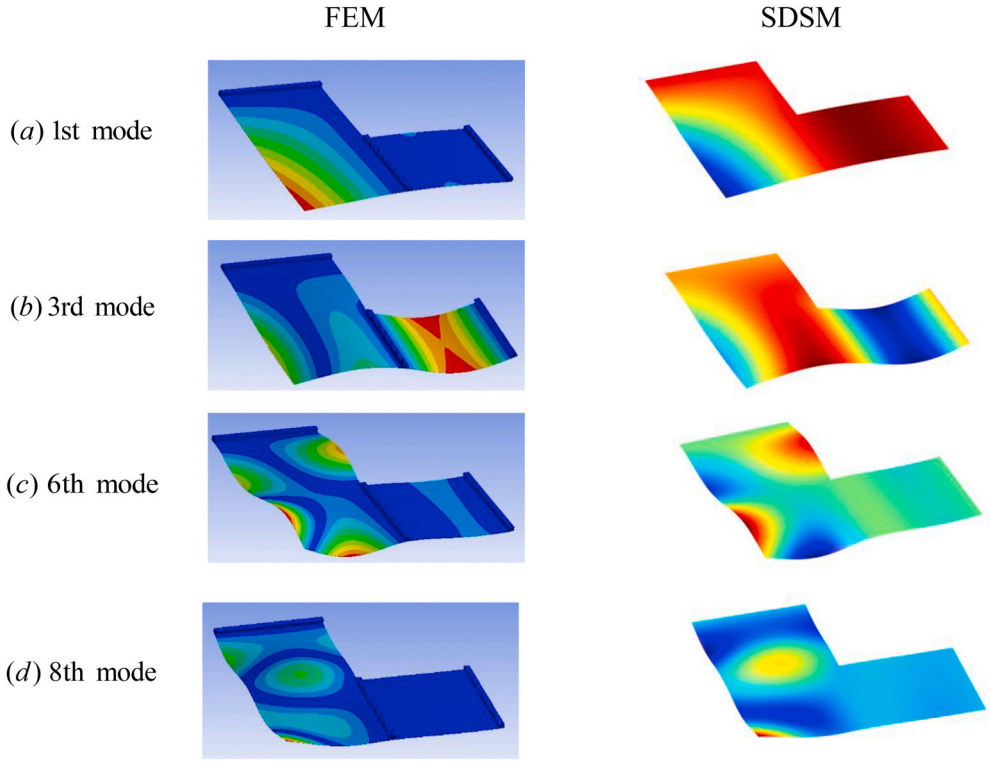

Fig. 18. Mode shapes of a stiffened L-shaped plate in Fig. 17 computed by FEM and SDSM.

Reviewing and Editing J. Ranjan Banerjee: Supervision, Writing-Reviewing and Editing.

Declaration of competing interest

The authors declare that they have no known competing financial interests or personal relationships that could have appeared to influence the work reported in this paper.

Acknowledgements

The authors appreciate the supports from the National Key R&D Program of China (Grant nos. 2018YFB1201600), National Natural Science Foundation (Grant No. 11802345, 51878667, 51678571), State Key Laboratory of High Performance Complex Manufacturing (Grant No. ZZYJKT2019-07) and Initial Funding of Specially-appointed Professorship (Grant No. 502045001) which made this research possible.

Appendix: Spectral dynamic stiffness method of the plate with arbitrary boundary conditions

This appendix record the spectral dynamic stiffness formulations [26,29] for a plate element with arbitrary boundary conditions as shown in Fig. 19. The size of the rectangular Kirchhoff plate is $2a \times 2b$, with a lateral displacement of $W(x,y)$. The frequency-dependent GDE is expressed as follows,

$$\frac{\partial^4 W}{\partial x^4} + 2\frac{\partial^4 W}{\partial x^2 \partial y^2} + \frac{\partial^4 W}{\partial y^4} - \kappa W = 0$$

where

$$\kappa = \frac{\rho h \omega^2}{D}, D = \frac{Eh^3}{12(1-\nu^2)}$$

in which, ω is the circular frequency, D is the bending stiffness of the plate, E is the Young's modulus of the material, ν is the Poisson's ratio, h and ρ are the thickness and mass density of the plate, respectively. The rotation, bending moment and shear force are as follows,

$$\psi_x = -\frac{\partial W}{\partial x}; \quad \psi_y = -\frac{\partial W}{\partial y};$$

$$M_x = -D\left(\frac{\partial^2 W}{\partial x^2} + \nu\frac{\partial^2 W}{\partial y^2}\right); \quad M_y = -D\left(\frac{\partial^2 W}{\partial y^2} + \nu\frac{\partial^3 W}{\partial x^2}\right);$$

$$V_x = -D\left(\frac{\partial^3 W}{\partial x^3} + \Gamma^*\frac{\partial^3 W}{\partial x \partial y^2}\right); V_y = -D\left(\frac{\partial^3 W}{\partial y^3} + \Gamma^*\frac{\partial^3 W}{\partial y \partial x^2}\right);$$

in which $\Gamma^* = 2-\nu$, M_x, V_x, ψ_x are the bending moment, shear force and rotation respectively at $x = \pm a$,and M_y, V_y, ψ_y are the bending moment, shear force and rotation angle respectively at$x = \pm b$.

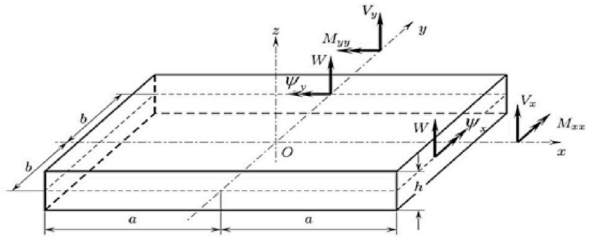

Fig. 19. Coordinate system and symbol of displacement and force of thin plate

According to the SDSM, the wavenumbers α_{km} and β_{jn} of the plate are as follows,

$$\alpha_{km} = \begin{cases} \dfrac{m\pi}{a} & k = 0 \\ \left(m + \dfrac{1}{2}\right)\dfrac{\pi}{a} & k = 1 \end{cases}, \quad \beta_{jn} = \begin{cases} \dfrac{n\pi}{b} & j = 0 \\ \left(n + \dfrac{1}{2}\right)\dfrac{\pi}{b} & j = 1 \end{cases}$$

Based on the SDSM as described in Refs. [26,29], the SDS formula expression forkj components are

$$\boldsymbol{f}^{kj} = \boldsymbol{K}^{kj}\boldsymbol{d}^{kj}$$

where $kj \in \{0,1\}$, denoting the symmetry of the four kj components, and

$$\boldsymbol{f}^{kj} = D\begin{bmatrix} \boldsymbol{V}^{kj} \\ \boldsymbol{M}^{kj} \end{bmatrix}, \quad \boldsymbol{d}^{kj} = \begin{bmatrix} \boldsymbol{W}^{kj} \\ \boldsymbol{\Psi}^{kj} \end{bmatrix}$$

$$\boldsymbol{K}^{kj} = D\begin{bmatrix} \boldsymbol{A}_{WN}^{kj\ -1} & -\boldsymbol{A}_{WW}^{kj\ -1}\boldsymbol{A}_{W\Phi}^{kj} \\ \boldsymbol{A}_{MV}^{kj}\boldsymbol{A}_{WV}^{kj\ -1} & \boldsymbol{A}_{M\Phi}^{kj} - \boldsymbol{A}_{MV}^{kj}\boldsymbol{A}_{WW}^{kj\ -1}\boldsymbol{A}_{W\varphi}^{kj} \end{bmatrix}$$

where $\boldsymbol{A}$ in the SDS component matrix $\boldsymbol{K}^{kj}$ has the following form, in which $m \in [0, M-1]$ and $n \in [0, N-1]$,

$$\boldsymbol{A}=\left[\begin{array}{ccc|ccc} \boldsymbol{A}(n,n)\big|_{n=0} & 0 & 0 & \boldsymbol{A}(n,m)\big|_{\substack{n=0\\m=0}} & \cdots & \boldsymbol{A}(n,m)\big|_{\substack{n=0\\m=N-1}} \\ 0 & \ddots & 0 & \vdots & \ddots & \vdots \\ 0 & 0 & \boldsymbol{A}(n,n)\big|_{n=N-1} & \boldsymbol{A}(n,m)\big|_{\substack{n=M-1\\m=0}} & \cdots & \boldsymbol{A}(n,m)\big|_{\substack{n=M-1\\m=N-1}} \\ \hline \boldsymbol{A}(m,n)\big|_{\substack{m=0\\n=0}} & \cdots & \boldsymbol{A}(m,n)\big|_{\substack{m=0\\n=N-1}} & \boldsymbol{A}(m,m)\big|_{m=0} & 0 & 0 \\ \vdots & \ddots & \vdots & 0 & \ddots & 0 \\ \boldsymbol{A}(m,n)\big|_{\substack{m=M-1\\n=0}} & \cdots & \boldsymbol{A}(m,n)\big|_{\substack{m=M-1\\n=N-1}} & 0 & 0 & \boldsymbol{A}(m,m)\big|_{m=M-1} \end{array}\right]$$

the terms of these four matrices can be expressed in a concise form as

$$A^{ij}_{W\psi}(n,n)=-(\Sigma_1\Upsilon_1-\Sigma_2\Upsilon_2)/\Upsilon_0 A^{kj}_{W\psi}(n,m)=-\Sigma_5\Sigma_7$$
$$A^{kj}_{W\psi}(m,n)=-\Sigma_6\Sigma_8 A^{kj}_{W\psi}(m,m)=-(\Sigma_3\Upsilon_3-\Sigma_4\Upsilon_4)/\Upsilon_0$$
$$A^{kj}_{WV}(n,n)=(\Upsilon_1-\Upsilon_2)/\Upsilon_0 A^{kj}_{WV}(n,m)=\Sigma_7$$
$$A^{kj}_{WV}(m,n)=\Sigma_8 A^{kj}_{WV}(m,m)=(\Upsilon_3-\Upsilon_4)/\Upsilon_0$$
$$A^{kj}_{M\psi}(n,n)=-\left(\Sigma_1^2\Upsilon_1-\Sigma_2^2\Upsilon_2\right)/\Upsilon_0 A^{kj}_{M\psi}(n,m)=-\Sigma_9\Sigma_7$$
$$A^{kj}_{M\psi}(m,n)=-\Sigma_9\Sigma_8 \qquad A^{kj}_{M\psi}(m,m)=-\left(\Sigma_3^2\Upsilon_3-\Sigma_4^2\Upsilon_4\right)/\Upsilon_0$$
$$A^{kj}_{MV}(n,n)=(\Sigma_1\Upsilon_1-\Sigma_2\Upsilon_2)/\Upsilon_0 \qquad A^{kj}_{MV}(n,m)=\Sigma_6\Sigma_7$$
$$A^{kj}_{MV}(m,n)=\Sigma_5\Sigma_8 \qquad A^{kj}_{MV}(m,m)=(\Sigma_3\Upsilon_3-\Sigma_4\Upsilon_4)/\Upsilon_0$$

where

$$r_0=2\sqrt{\kappa},\quad \Sigma_0=2(-1)^{m+n}$$
$$\Upsilon_1=\mathscr{T}\mathscr{H}_k\left(q_{1jn}a\right)/q_{1jn},\quad \Upsilon_2=\mathscr{T}\mathscr{H}_k\left(q_{2jn}a\right)/q_{2jn}$$
$$\Upsilon_3=\mathscr{T}\mathscr{H}_j(p_{1km}b)/p_{1km},\quad \Upsilon_4=\mathscr{T}\mathscr{H}_j(p_{2km}b)/p_{2km}$$
$$\Sigma_1=\nu\beta_{jn}^2-q_{1jn}^2,\quad \Sigma_2=\nu\beta_{jn}^2-q_{2jn}^2$$
$$\Sigma_3=\nu\alpha_{km}^2-p_{1km}^2,\quad \Sigma_4=\nu\alpha_{km}^2-p_{2km}^2$$
$$\Sigma_5=\nu\alpha_{km}^2+\beta_{jn}^2,\quad \Sigma_6=\alpha_{km}^2+\nu\beta_{jn}^2$$
$$\Sigma_7=\Sigma_0\Big/\left[\sqrt{\zeta_{jn}\zeta_{km}}ab\left(p_{1km}^2+\beta_{jn}^2\right)\left(p_{2km}^2+\beta_{\mathrm{jn}}^2\ \right)\right]$$
$$\Sigma_8=\Sigma_0\Big/\left[\sqrt{\zeta_{jn}\zeta_{km}}ab\left(q_{1jn}^2+\alpha_{km}^2\right)\left(q_{2jn}^2+\alpha_{km}^2\right)\right]$$
$$\Sigma_9=(1-\nu)^2\alpha_{km}^2\beta_{jn}^2+\nu\kappa$$

where

$$T\mathscr{H}_l(\Xi)=\mathscr{H}_l(\Xi)\Big/\mathscr{H}^*_l(\Xi),\ \mathscr{H}_i(\Gamma\xi)=\begin{cases}\cosh(\Gamma\xi), & l=0\\ \sinh(\Gamma\xi), & l=1\end{cases}$$

$$p_{1bm}=\sqrt{\alpha_{km}^2-\sqrt{\kappa}},p_{2km}=\sqrt{\alpha_{km}^2+\sqrt{\kappa}},\ q_{1jn}=\sqrt{\beta_{jn}^2-\sqrt{\kappa}},q_{2jn}=\sqrt{\beta_{jn}^2+\sqrt{\kappa}}$$

Assembling the*kj*component matrix$\boldsymbol{K}^{kj}$into the SDS matrix of the plate element $\boldsymbol{K}_P$as follows,

$$\boldsymbol{K}_P=\frac{1}{2}\boldsymbol{T}\begin{bmatrix}\boldsymbol{K}^{00} & \boldsymbol{0} & \boldsymbol{0} & \boldsymbol{0}\\ \boldsymbol{0} & \boldsymbol{K}^{01} & \boldsymbol{0} & \boldsymbol{0}\\ \boldsymbol{0} & \boldsymbol{0} & \boldsymbol{K}^{10} & \boldsymbol{0}\\ \boldsymbol{0} & \boldsymbol{0} & \boldsymbol{0} & \boldsymbol{K}^{11}\end{bmatrix}\boldsymbol{T}^T$$

where $\boldsymbol{T}$ is the total transfer matrix, the analytical formula is as follows,

$$T=\begin{bmatrix}
\boldsymbol{I}_n & \boldsymbol{O} & \boldsymbol{O} & \boldsymbol{O} & \boldsymbol{O} & \boldsymbol{O} & \boldsymbol{O} & \boldsymbol{O} & \boldsymbol{I}_n & \boldsymbol{O} & \boldsymbol{O} & \boldsymbol{O} & \boldsymbol{O} & \boldsymbol{O} & \boldsymbol{O} & \boldsymbol{O} \\
\boldsymbol{O} & \boldsymbol{O} & \boldsymbol{O} & \boldsymbol{O} & \boldsymbol{I}_n & \boldsymbol{O} & \boldsymbol{O} & \boldsymbol{O} & \boldsymbol{O} & \boldsymbol{O} & \boldsymbol{O} & \boldsymbol{O} & \boldsymbol{I}_n & \boldsymbol{O} & \boldsymbol{O} & \boldsymbol{O} \\
\boldsymbol{O} & \boldsymbol{I}_n & \boldsymbol{O} & \boldsymbol{O} & \boldsymbol{O} & \boldsymbol{O} & \boldsymbol{O} & \boldsymbol{O} & \boldsymbol{O} & \boldsymbol{I}_n & \boldsymbol{O} & \boldsymbol{O} & \boldsymbol{O} & \boldsymbol{O} & \boldsymbol{O} & \boldsymbol{O} \\
\boldsymbol{O} & \boldsymbol{O} & \boldsymbol{O} & \boldsymbol{O} & \boldsymbol{O} & \boldsymbol{I}_n & \boldsymbol{O} & \boldsymbol{O} & \boldsymbol{O} & \boldsymbol{O} & \boldsymbol{O} & \boldsymbol{O} & \boldsymbol{O} & \boldsymbol{I}_n & \boldsymbol{O} & \boldsymbol{O} \\
\boldsymbol{O} & \boldsymbol{O} & \boldsymbol{I}_m & \boldsymbol{O} & \boldsymbol{O} & \boldsymbol{O} & \boldsymbol{I}_m & \boldsymbol{O} & \boldsymbol{O} & \boldsymbol{O} & \boldsymbol{O} & \boldsymbol{O} & \boldsymbol{O} & \boldsymbol{O} & \boldsymbol{O} & \boldsymbol{O} \\
\boldsymbol{O} & \boldsymbol{O} & \boldsymbol{O} & \boldsymbol{O} & \boldsymbol{O} & \boldsymbol{O} & \boldsymbol{O} & \boldsymbol{O} & \boldsymbol{O} & \boldsymbol{O} & \boldsymbol{I}_m & \boldsymbol{O} & \boldsymbol{O} & \boldsymbol{O} & \boldsymbol{I}_m & \boldsymbol{O} \\
\boldsymbol{O} & \boldsymbol{O} & \boldsymbol{O} & \boldsymbol{I}_m & \boldsymbol{O} & \boldsymbol{O} & \boldsymbol{O} & \boldsymbol{I}_m & \boldsymbol{O} & \boldsymbol{O} & \boldsymbol{O} & \boldsymbol{O} & \boldsymbol{O} & \boldsymbol{O} & \boldsymbol{O} & \boldsymbol{O} \\
\boldsymbol{O} & \boldsymbol{O} & \boldsymbol{O} & \boldsymbol{O} & \boldsymbol{O} & \boldsymbol{O} & \boldsymbol{O} & \boldsymbol{O} & \boldsymbol{O} & \boldsymbol{O} & \boldsymbol{O} & \boldsymbol{I}_m & \boldsymbol{O} & \boldsymbol{O} & \boldsymbol{O} & \boldsymbol{I}_m \\
\boldsymbol{I}_n & \boldsymbol{O} & \boldsymbol{O} & \boldsymbol{O} & \boldsymbol{O} & \boldsymbol{O} & \boldsymbol{O} & \boldsymbol{O} & -\boldsymbol{I}_n & \boldsymbol{O} & \boldsymbol{O} & \boldsymbol{O} & \boldsymbol{O} & \boldsymbol{O} & \boldsymbol{O} & \boldsymbol{O} \\
\boldsymbol{O} & \boldsymbol{O} & \boldsymbol{O} & \boldsymbol{O} & \boldsymbol{I}_n & \boldsymbol{O} & \boldsymbol{O} & \boldsymbol{O} & \boldsymbol{O} & \boldsymbol{O} & \boldsymbol{O} & \boldsymbol{O} & -\boldsymbol{I}_n & \boldsymbol{O} & \boldsymbol{O} & \boldsymbol{O} \\
\boldsymbol{O} & -\boldsymbol{I}_n & \boldsymbol{O} & \boldsymbol{O} & \boldsymbol{O} & \boldsymbol{O} & \boldsymbol{O} & \boldsymbol{O} & \boldsymbol{O} & \boldsymbol{I}_n & \boldsymbol{O} & \boldsymbol{O} & \boldsymbol{O} & \boldsymbol{O} & \boldsymbol{O} & \boldsymbol{O} \\
\boldsymbol{O} & \boldsymbol{O} & \boldsymbol{O} & \boldsymbol{O} & \boldsymbol{O} & -\boldsymbol{I}_n & \boldsymbol{O} & \boldsymbol{O} & \boldsymbol{O} & \boldsymbol{O} & \boldsymbol{O} & \boldsymbol{O} & \boldsymbol{O} & \boldsymbol{I}_n & \boldsymbol{O} & \boldsymbol{O} \\
\boldsymbol{O} & \boldsymbol{O} & \boldsymbol{I}_m & \boldsymbol{O} & \boldsymbol{O} & \boldsymbol{O} & -\boldsymbol{I}_m & \boldsymbol{O} & \boldsymbol{O} & \boldsymbol{O} & \boldsymbol{O} & \boldsymbol{O} & \boldsymbol{O} & \boldsymbol{O} & \boldsymbol{O} & \boldsymbol{O} \\
\boldsymbol{O} & \boldsymbol{O} & \boldsymbol{O} & \boldsymbol{O} & \boldsymbol{O} & \boldsymbol{O} & \boldsymbol{O} & \boldsymbol{O} & \boldsymbol{O} & \boldsymbol{O} & \boldsymbol{I}_m & \boldsymbol{O} & \boldsymbol{O} & \boldsymbol{O} & -\boldsymbol{I}_m & \boldsymbol{O} \\
\boldsymbol{O} & \boldsymbol{O} & \boldsymbol{O} & -\boldsymbol{I}_m & \boldsymbol{O} & \boldsymbol{O} & \boldsymbol{O} & \boldsymbol{I}_m & \boldsymbol{O} & \boldsymbol{O} & \boldsymbol{O} & \boldsymbol{O} & \boldsymbol{O} & \boldsymbol{O} & \boldsymbol{O} & \boldsymbol{O} \\
\boldsymbol{O} & \boldsymbol{O} & \boldsymbol{O} & \boldsymbol{O} & \boldsymbol{O} & \boldsymbol{O} & \boldsymbol{O} & \boldsymbol{O} & \boldsymbol{O} & \boldsymbol{O} & \boldsymbol{O} & -\boldsymbol{I}_m & \boldsymbol{O} & \boldsymbol{O} & \boldsymbol{O} & \boldsymbol{I}_m
\end{bmatrix}$$

where $\boldsymbol{I}_m$ and $\boldsymbol{I}_n$ are n-dimensional and m-dimensional identity matrices respectively, and $\boldsymbol{O}$ represents an empty matrix.

References

[1] J.S. Lee, E. Deckers, S. Jonckheere, W. Desmet, Y.Y. Kim, A direct hybrid finite element-wave based modelling technique for efficient analysis of poroelastic materials in steady-state acoustic problems[J], Comput. Methods Appl. Mech. Eng. 304 (2016) 55–80.

[2] R.S. Langley, V. Cotoni, Response variance prediction in the statistical energy analysis of built-up systems[J], J. Acoust. Soc. Am. 115 (2) (2004) 706–718.

[3] Vergote K, Vandepitte D, Desmet W. On the use of a hybrid wave based-statistical energy approach for the analysis of vibro-acoustic systems in the mid-frequency range[J]. Proceedings of ISMA 2010 - International Conference on Noise and Vibration Engineering, Including USD 2010, 2010(January): 2437–2449.

[4] I. Elishakoff, A. Sternberg, Vibration of rectangular plates with edge-beams[J], Acta Mech. 36 (1980) 195–212.

[5] B.R. Mace, Sound radiation from fluid loaded stiffened[J], J. Sound Vib. 79 (1981) 439–452.

[6] B.R. Mace, Sound radiation from a plate reinforced by two sets of parallel stiffeners [J], J. Sound Vib. 71 (3) (1980) 435–441.

[7] D.J. Mead, Plates with regular stiffening in acoustic media: vibration and radiation [J], J. Acoust. Soc. Am. 88 (1) (1990) 391–401.

[8] X.W. Yin, X.J. Gu, H.F. Cui, R.Y. Shen, Acoustic radiation from a laminated composite plate reinforced by doubly periodic parallel stiffeners[J], J. Sound Vib. 306 (3–5) (2007) 877–889.

[9] Z. Siddiqi, A. Kukreti, Analysis of eccentrically stiffened plates with mixed boundary conditions using differential quadrature method[J], Appl. Math. Model. 22 (4–5) (1998) 251–275.

[10] C. Mittelstedt, Explicit local buckling analysis of stiffened composite plates accounting for periodic boundary conditions and stiffener-plate interaction[J], Compos. Struct. 91 (3) (2009) 249–265.

[11] H. Xu, J. Du, W.L. Li, Vibrations of rectangular plates reinforced by any number of beams of arbitrary lengths and placement angles[J], J. Sound Vib. 329 (18) (2010) 3759–3779.

[12] X. Zhang, W.L. Li, A unified approach for predicting sound radiation from baffled rectangular plates with arbitrary boundary conditions[J], J. Sound Vib. 329 (25) (2010) 5307–5320.

[13] T.R. Lin, An analytical and experimental study of the vibration response of a clamped ribbed plate[J], J. Sound Vib. 331 (4) (2012) 902–913.

[14] T.R. Lin, K. Zhang, An analytical study of the free and forced vibration response of a ribbed plate with free boundary conditions[J], J. Sound Vib. 422 (2018) 15–33.

[15] M. Golkaram, M.M. Aghdam, Free transverse vibration analysis of thin rectangular plates locally suspended on elastic beam[J], Proc. IME C J. Mech. Eng. Sci. 227 (7) (2013) 1515–1524.

[16] D.J. Gorman, Free vibration analysis of corner-supported rectangular plates with symmetrically distributed edge beams[J], J. Sound Vib. 263 (5) (2003) 979–1003.

[17] H. Zheng, Z. Wei, Vibroacoustic analysis of stiffened plates with nonuniform boundary conditions[J], International Journal of Applied Mechanics 5 (4) (2013) 1–19.

[18] O. Aksogan, C.D. Turkozer, E. Emsen, R. Resatoglu, Dynamic analysis of non-planar coupled shear walls with stiffening beams using Continuous Connection Method [J], Thin-Walled Struct. 82 (2014) 95–104.

[19] Q. Huang, R. Xu, Y. Liu, H. Hu, G. Giunta, S. Belouettar, M. Potier-Ferry, A two-dimensional Fourier-series finite element for wrinkling analysis of thin films on compliant substrates[J], Thin-Walled Struct. 114 (2017) 144–153.

[20] W. Huang, Q. Huang, Y. Liu, J. Yang, H. Hu, F. Trochu, P. Causse, A Fourier based reduced model for wrinkling analysis of circular membranes[J], Comput. Methods Appl. Mech. Eng. 345 (2019) 1114–1137.

[21] Q. Huang, Y. Liu, H. Hu, Q. Shao, K. Yu, G. Giunta, S. Belouettar, M. Potier-Ferry, A Fourier-related double scale analysis on the instability phenomena of sandwich plates[J], Comput. Methods Appl. Mech. Eng. 318 (2017) 270–295.

[22] L. Liu, J.M. Li, G.A. Kardomateas, Nonlinear vibration of a composite plate to harmonic excitation with initial geometric imperfection in thermal environments [J], Compos. Struct. 209 (2019) 401–423.

[23] J. Li, B. Zhao, H. Cheng, G. Kardomateas, L. Liu, Nonlinear dynamic response of a sandwich structure with flexible core in thermal environments[J], J. Sandw. Struct. Mater. (2020) 1–36.

[24] B. Qin, R. Zhong, T. Wang, Q. Wang, Y. Xu, Z. Hu, A unified Fourier series solution for vibration analysis of FG-CNTRC cylindrical, conical shells and annular plates with arbitrary boundary conditions[J], Compos. Struct. 232 (2020) 111549.

[25] B. Qin, Q. Wang, R. Zhong, X. Zhao, C. Shuai, A three-dimensional solution for free vibration of FGP-GPLRC cylindrical shells resting on elastic foundations: a comparative and parametric study[J], Int. J. Mech. Sci. 187 (2020) 105896.

[26] T. Liu, A. Wang, Q. Wang, B. Qin, Wave based method for free vibration characteristics of functionally graded cylindrical shells with arbitrary boundary conditions[J], Thin-Walled Struct. 148 (2020) 106580.

[27] X. Liu, C. Sun, J.R. Banerjee, H.-C. Dan, L. Chang, An exact dynamic stiffness method for multibody systems consisting of beams and rigid-bodies[J], Mech. Syst. Signal Process. 150 (2021) 107264.

[28] W.H. Wittrick, F.W. Williams, Buckling and vibration of anisotropic or isotropic plate assemblies under combined loadings[J], Int. J. Mech. Sci. 16 (4) (1974) 209–239.

[29] M. Boscolo, J.R. Banerjee, Dynamic stiffness method for exact inplane free vibration analysis of plates and plate assemblies[J], J. Sound Vib. 330 (12) (2011) 2928–2936.

[30] D. Tounsi, J.B. Casimir, S. Abid, I. Tawfiq, M. Haddar, Dynamic stiffness formulation and response analysis of stiffened shells[J], Comput. Struct. 132 (2014) 75–83.

[31] F.A. Fazzolari, A refined dynamic stiffness element for free vibration analysis of cross-ply laminated composite cylindrical and spherical shallow shells[J], Compos. B Eng. 62 (2014) 143–158.

[32] H. Li, X. Yin, W. Wu, Dynamic stiffness formulation for in-plane and bending vibrations of plates with two opposite edges simply supported[J], J. Vib. Contr. 24 (9) (2016) 1652–1669.

[33] X. Liu, X. Zhao, C. Xie, Exact free vibration analysis for membrane assemblies with general classical boundary conditions[J], J. Sound Vib. (2020) 115484.

[34] X. Liu, C. Xie, H.-C. Dan, Exact free vibration analysis for plate built-up structures under comprehensive combinations of boundary conditions[J], Shock Vib. 2020 (2020) 1–21, 5305692.

[35] R.S. Langley, Application of the dynamic stiffness method to the free and forced vibrations of aircraft panels[J], J. Sound Vib. 135 (2) (1989) 319–331.

[36] R.S. Langley, A dynamic stiffness technique for the vibration analysis of stiffened shell structures[J], J. Sound Vib. 156 (3) (1992) 521–540.

[37] A. Watson, D. Kennedy, F.W. Williams, C.A. Featherston, Buckling and vibration of stiffened panels or single plates with clamped ends[J], Adv. Struct. Eng. 6 (2) (2003) 135–144.

[38] X. Yin, W. Wu, K. Zhong, H. Li, Dynamic stiffness formulation for the vibrations of stiffened plate structures with consideration of in-plane deformation[J], J. Vib. Contr. 24 (20) (2018) 4825–4838.

[39] X. Liu, J.R. Banerjee, Free vibration analysis for plates with arbitrary boundary conditions using a novel spectral-dynamic stiffness method[J], Comput. Struct. 164 (2016) 108–126.

[40] X. Liu, J.R. Banerjee, An exact spectral-dynamic stiffness method for free flexural vibration analysis of orthotropic composite plate assemblies - Part II: applications [J], Compos. Struct. 132 (2015) 1274–1287.

[41] X. Liu, J.R. Banerjee, The spectral-dynamic stiffness method: a novel approach for exact free vibration analysis of plate-like structures[J], Civil-Comp Proceedings, 2015.

[42] S.O. Papkov, J.R. Banerjee, Dynamic stiffness formulation and free vibration analysis of specially orthotropic Mindlin plates with arbitrary boundary conditions [J], J. Sound Vib. 458 (2019) 522–543.

[43] X. Liu, J.R. Banerjee, A spectral dynamic stiffness method for free vibration analysis of plane elastodynamic problems[J], Mech. Syst. Signal Process. 87 (2017) 136–160.
[44] X. Liu, H.I. Kassem, J.R. Banerjee, An exact spectral dynamic stiffness theory for composite plate-like structures with arbitrary non-uniform elastic supports, mass attachments and coupling constraints[J], Compos. Struct. 142 (2016) 140–154.
[45] X. Liu, Spectral dynamic stiffness formulation for inplane modal analysis of composite plate assemblies and prismatic solids with arbitrary classical/nonclassical boundary conditions[J], Compos. Struct. 158 (2016) 262–280.
[46] X. Liu, X. Liu, W. Zhou, An analytical spectral stiffness method for buckling of rectangular plates on Winkler foundation subject to general boundary conditions [J], Applied Mathematical Modelling, 2020.
[47] X. Liu, X. Liu, S. Xie, A highly accurate analytical spectral flexibility formulation for buckling and wrinkling of orthotropic rectangular plates[J], Int. J. Mech. Sci. 168 (2020), 105311.
[48] M. Nefovska-Danilovic, M. Petronijevic, In-plane free vibration and response analysis of isotropic rectangular plates using the dynamic stiffness method[J], Comput. Struct. 152 (2015) 82–95.
[49] N. Kolarevic, M. Nefovska-Danilovic, M. Petronijevic, Dynamic stiffness elements for free vibration analysis of rectangular Mindlin plate assemblies[J], Journal of sound and vibration, Elsevier 359 (2015) 84–106.
[50] N. Kolarevic, M. Marjanović, M. Nefovska-Danilovic, M. Petronijevic, Free vibration analysis of plate assemblies using the dynamic stiffness method based on the higher order shear deformation theory[J], J. Sound Vib. 364 (2016) 110–132.
[51] X. Liu, J.R. Banerjee, An exact spectral-dynamic stiffness method for free flexural vibration analysis of orthotropic composite plate assemblies - Part I: theory[J], Compos. Struct. 132 (2015) 1274–1287.
[52] D. Wang, S. Xie, Z. Feng, X. Liu, Y. Li, Investigating the effect of dimension parameters on sound transmission losses in nomex honeycomb sandwich[J], Appl. Sci. 10 (9) (2020) 3109.
[53] S. Xie, S. Yang, C. Yang, D. Wang, Sound absorption performance of a filled honeycomb composite structure[J], Appl. Acoust. 162 (2020) 107202.
[54] S. Xie, D. Wang, Z. Feng, S. Yang, Sound absorption performance of microperforated honeycomb metasurface panels with a combination of multiple orifice diameters, [J]. Applied Acoustics 158 (2020) 107046.
[55] S. Xie, K. Jing, H. Zhou, X. Liu, Mechanical properties of Nomex honeycomb sandwich panels under dynamic impact[J], Composite Structures, Elsevier 235 (October 2019) (2020) 111814.
[56] Y. Li, Y. Zhang, S. Xie, A lightweight multilayer honeycomb membrane-type acoustic metamaterial[J], Appl. Acoust. 168 (2020) 107427.
[57] Y. Li, Y. Wang, S. Yao, Multipolar resonance and bandgap formation mechanism of star-shaped lattice structure[J], Int. J. Mech. Sci. (2020) 106163.
[58] Y. Li, H. Li, Bandgap merging and widening of elastic metamaterial with heterogeneous resonator[J], J. Phys. Appl. Phys. 53 (47) (2020) 475302.
[59] F.W. Williams, Z. Wanxie, P.N. Bennett, Computation of the eigenvalues of wave propagation in periodic substructural systems[J], J. Vib. Acoust. 115 (4) (1993) 422–426.
[60] L. Jiang, X. Liu, P. Xiang, W. Zhou, Train-bridge system dynamics analysis with uncertain parameters based on new point estimate method[J], Eng. Struct. 199 (2019) 109454.